The Economic and Environmental Cost of Pirate Avoidance

November 18, 2025

- Renato Molina^{1,2*}, Juan Carlos Villaseñor-Derbez^{1,3}, Gavin McDonald^{4,5,6}, Grant McDermott⁷
- ⁶ Department of Environmental Science and Policy, Rosenstiel School of Marine, Atmospheric, and
- ⁷ Earth Science, University of Miami

3

17

18

19

20

21

22

23

24

25

26

27

28

- ⁸ Department of Economics, University of Miami
- ³Frost Institute for Data Science and Computing, University of Miami
- ¹⁰ ⁴Marine Science Institute, University of California, Santa Barbara
- ¹¹ ⁵Bren School of Environmental Science & Management, University of California, Santa Barbara
- ⁶Environmental Markets Lab, University of California, Santa Barbara
- ⁷Department of Economics, University of Oregon
- *To whom correspondence should be addressed; E-mail: renato.molina@miami.edu.

16 Abstract

Modern-day piracy is a pervasive problem for the global maritime industry, yet its economic costs are largely unquantified. We address this gap by pairing a detailed dataset of pirate encounters with satellite tracking information of more than 26 million shipping voyages from 2012 to 2023. Our analysis reveals clear patterns of avoidance behavior following piracy attacks, leading to increased travel costs of US\$1.3 billion annually. Accounting for environmental damages from harmful emissions adds another US\$4.1 billion in annual welfare losses. These estimates highlight the substantial cost imposed by piracy on international maritime operations, as well as the potential benefit from global anti-piracy measures, which we estimate could be funded at a fraction of current losses.

1 Introduction

Oceans have served as the main conduit of global trade for centuries. Today, maritime transport carries more than 70% of the world's traded goods by value and more than 80% by volume

[4]. Yet the transportation of valuable goods has always created opportunities for predation. Maritime routes are particularly vulnerable because they are poorly enforced, and isolated vessels make ideal targets for ambush and escape. The frequent lack of legal jurisdictions further complicates capture and prosecution. Thus, and despite its common historical associations, maritime piracy remains a significant problem today.¹

Official records list more than 2,600 global pirate encounters between 2012 and 2023, with 166 taking place in 2023 alone (Figure 1). Most of these encounters concentrate in busy trade channels, where pirates target high-value vessels for robbery or capture-to-ransom [23]. Panel A of Figure 1 highlights three "hotspots"—the Gulf of Aden, the Gulf of Guinea, and the Malacca Strait in Southeast Asia—where pirate encounters have been particularly acute.

Despite the prevalence of maritime piracy, there is relatively little research on its welfare impacts. Previous efforts to quantify the cost of the problem suggest annual losses in excess of US\$20 billion/year [12, 8]. However, the mechanics underlying these costs are not always clearly specified and the welfare estimates are derived from aggregate insurance records; see Supplementary Information A for a detailed literature review and additional background on global piracy. In this paper, we take a different approach by constructing micro-founded estimates of piracy costs from observed vessel behavior. By pairing detailed piracy encounter data with satellite tracking of more than 26 million individual shipping voyages from 2012 to 2023, we quantify how vessels adjust their routes in response to piracy threats. These behavioral responses allow us to derive bottom-up estimates of both the direct economic costs from increased travel distances and the environmental costs from additional emissions.

Our paper makes two distinct contributions. First, we identify and empirically measure avoidance shipping behavior on a rich dataset that combines detailed voyage information with pirate encounters. Second, we quantify the implied aggregate costs that can be attributed to piracy and the ripple effects on vessel behavior and global shipping. The novel dataset leveraged in this analysis includes high resolution spatio-temporal information on pirate encounters

¹Historians point out that piracy often follows a well-defined cycle involving a group of individuals from impoverished coastal areas that would band to predate on small-scale, poorly enforced shipments. These groups would then transition to a state of adjustment, for which "competition" dictates profitability and thereby their longevity in the piracy business [2, 19]. Most of these observations are based on pirates from previous centuries, but the resemblance with modern pirates is evident. See Bahadur [7] and Bueger [11] for a detailed account of the cycle and organizational mechanisms in the case of the pirates of Somalia, which resembles very closely the documented paths for earlier pirates. A similar analysis of piracy in the Gulf of Guinea has been done by Kamal [28].

Α

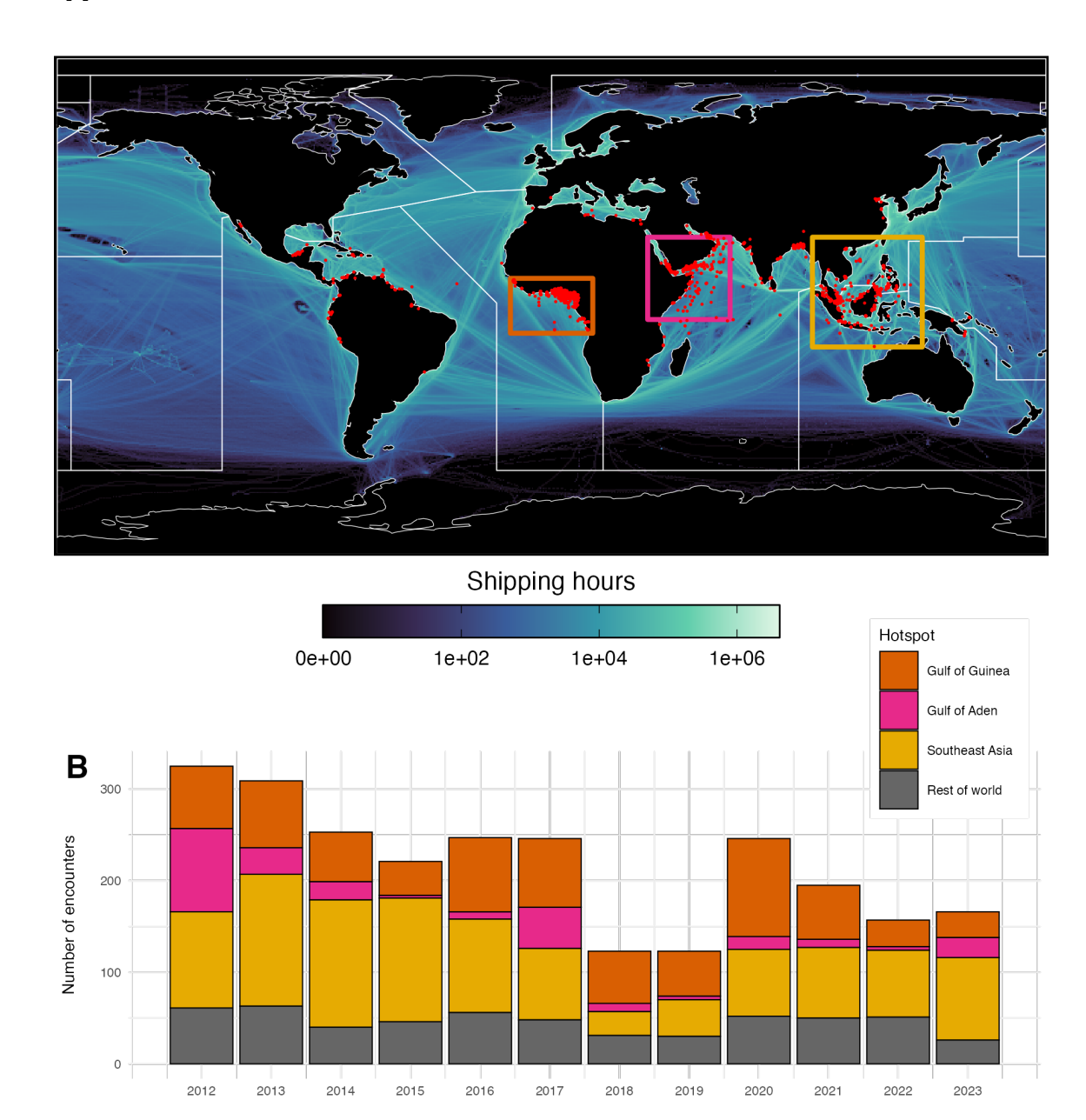


Figure 1: A global view of modern-day maritime transport and piracy. Panel A shows the spatial overlap of shipping activity and pirate encounters from 2012 to 2023. Note that data are \log_{10} -transformed for visualization purposes and represented using a $0.5^{\circ} \times 0.5^{\circ}$ grid in geographic coordinates, with the fill color of each pixel representing the total shipping transit time from 2012-2023 (hr). Pirate encounters are shown as red points. The colored overlay bounding rectangles correspond to the three main piracy hotspots, namely: 1) Gulf of Guinea, 2) Gulf of Aden, and 3) Southeast Asia. The bounding boxes are defined by an empirical density-based clustering approach (see Materials and Methods). Outlines of the major Anti-shipping Activity Messages (ASAM) regions are shown as white lines. Panel B shows the number of pirate encounters across hotspots and the rest of the world from 2012 to 2023.

from the US National Geospatial Intelligence Agency ASAM database [38], as well as individual vessel tracks of all known cargo, tanker, and refrigerated vessels that use the Automatic Identification System (AIS) globally [1]. Our empirical results show that a pirate encounter diverts maritime traffic away from the area of an encounter for about 6 days after the report is filed. These adjustments, along a shipping route, are associated with trips being extended by an average of 65 (± 13) kilometers. When aggregated at the global level, and taking into account prevailing fuel and labor costs, these adjustments suggest additional transportation costs of US\$1.7 billion during 2023 (annual average 2012-2023 of US\$1.3 B). Moreover, we estimate that surplus emission of air pollutants (CO₂, NO_x, and SO_x) due to increased fuel usage yield an additional US\$4.1 billion in environmental damages.

2 Results

2.1 A case study in piracy avoidance

To avoid ambiguity, it will prove helpful to define precisely several terms that we use in our analysis. A route is a port-to-port combination, a voyage is a trip made along a route, and a path is the sequence of coordinates chosen by the vessel to travel a route. With these definitions in hand, let us consider a case study of how individual vessels can best respond to the threat of piracy. Specifically, how should shippers respond to information about pirate presence along their route? We can reasonably assume that deterrence and enforcement options are too costly for most individual vessels to bear. As such, adaptation provides the best course of action.

Figure 2 depicts the behavioral response to a 2013 pirate attack in the Makassar Strait near Indonesia. On June 19, a Hong Kong-flagged bulk carrier was boarded by several pirates. News about the encounter was immediately broadcast to other vessels in the region via the Anti-shipping Activity Messages (ASAM) communication network, a global service provided by the United States Office of Naval Intelligence [36]. ² This information allowed the vessels to rapidly adjust their behavior; we observe a near-total avoidance of the encounter area

²The Worldwide Threat to Shipping Report reads: On 19 June, the anchored Hong Kong-flagged bulk carrier OCEAN GARNET was boarded at 01:11 S – 117:12 E, at the Muara Jawa Anchorage, Samarinda. Deck watch keepers onboard the anchored bulk carrier noticed three to five robbers with long knives near the forecastle store. They raised the alarm and retreated into the accommodation. On hearing the alarm, the robbers escaped in their waiting boat. Upon investigation, it was discovered that ship's stores had been stolen. Port control was informed. [36]

following the ASAM broadcast. The previous cluster of shipping activity near the Muara Jawa Anchorage—marked by a red "X" on the map—all but disappears and is replaced by a new one further South (Panel A). The number of voyages in the affected area also drops from an average of 48 per day to just 3 per day (Panel B).

2.2 Quantifying global avoidance behavior

80

81

82

83

85

86

87

88

90

91

92

93

94

95

96

97

98

99

100

101

102

103

104

105

106

107

108

Figure 2 provides *prima facie* evidence of avoidance behavior following a single piracy event. In this section, we expand our analysis to the global level and quantify the extent to which shippers take adaptive measures to avoid areas of active pirate risk. Formally, we test whether vessel traffic changes after a piracy encounter becomes public knowledge using two different empirical approaches.

First, we examine adaptation over space where *space* is the unit of observation. Just as we saw in the Makassar Strait example, this implies a behavioral adjustment that yields fewer transits through a region after an attack. We evaluate this prediction formally by testing for systematic changes in daily transit activity within all $0.5^{\circ} \times 0.5^{\circ}$ grid cells that experienced reported pirate activity between 2012 and 2023. The results are summarized as a series of event study plots in Figure 3 (see Supplementary Information B for detailed regression tables). We find that vessel activity is significantly reduced in the week following a pirate encounter. This finding holds for analyzes of global data across a variety of transit measures. Specifically, we estimate that a piracy event causes a 6-7% drop in average occupancy time (Panel A) and a 7-15% drop in total distance traveled (Panel B) within an affected cell. The analysis in the subsequent panels shows that this effect is driven by a reduction in the number of vessels and trips transiting through a grid cell, rather than by behavioral adjustments within a grid cell (e.g., vessels taking shorter paths within a cell; see Panel F). Our results are robust to various specification tests such as a change in grid resolution, as well as behavioral confounders such as shippers disabling their AIS transponders (an emergency safety measure officially allowed by the International Maritime Organization if a captain fears their ship is in danger of piracy [39]). See Supplementary Information D.1 for more information about these robustness checks.

For our second approach, we examine individual voyages. Here we are interested in how the avoidance behavior manifests at the level of individual voyages. Our results from Figure 3

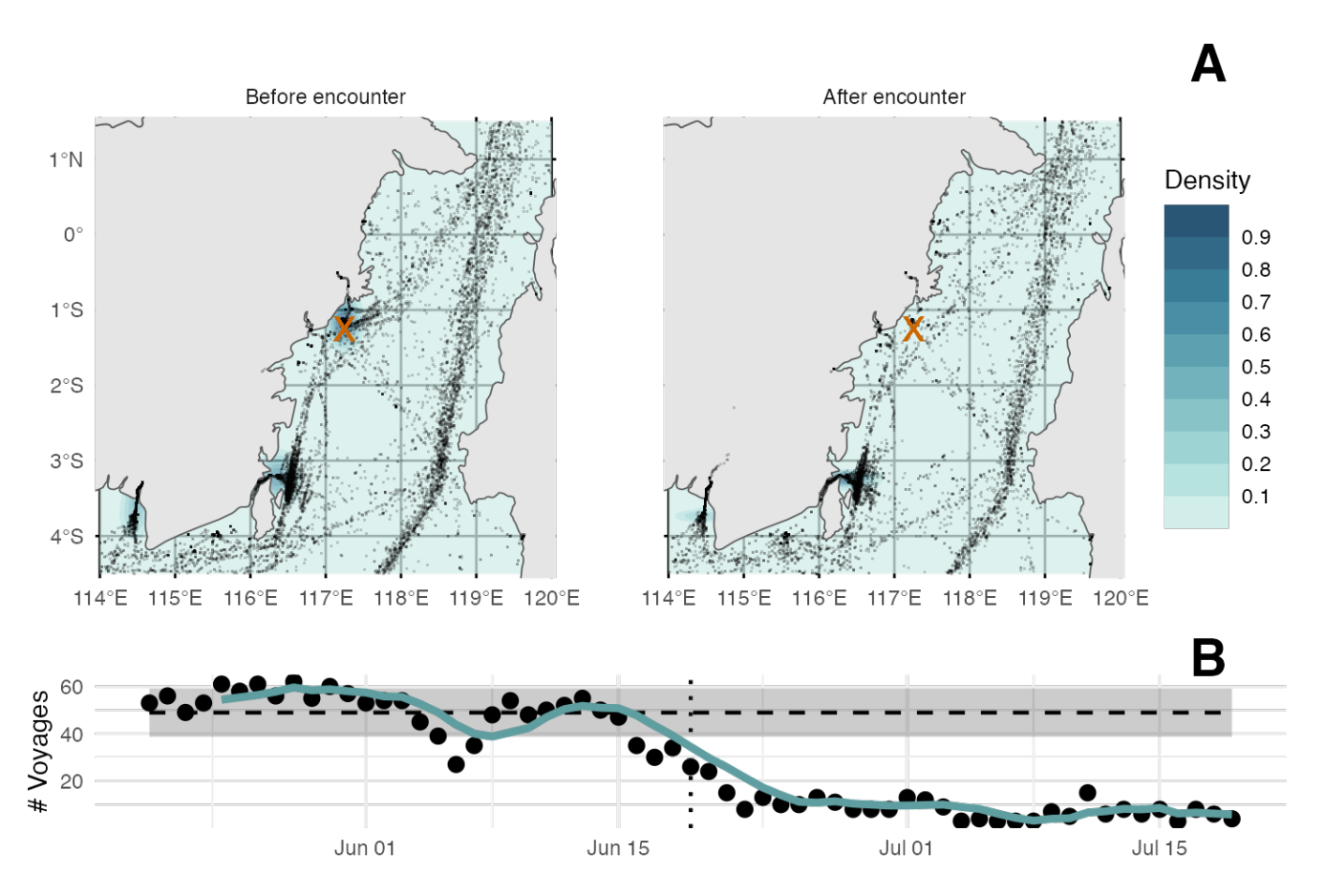


Figure 2: Example of change in shipping vessel transit following an encounter with pirates on June 19, 2013 off the coast of Indonesia. Panel A shows maps of the Muara Jawa Anchorage one week before (left) and after (right) the pirate encounter. Black points show vessel positions, and background colors show a 2-dimensional kernel estimate of vessel density. Panel B shows a time series of daily number of voyages crossing the affected pixel (at 117E, 1.5S, indicated with an orange "X" in A). Each point shows the total daily number of voyages, and the blue line shows the mean number in a 5-day rolling window. The horizontal dashed line and shaded area show the baseline number of daily voyages (mean \pm standard-deviation) before the attack.

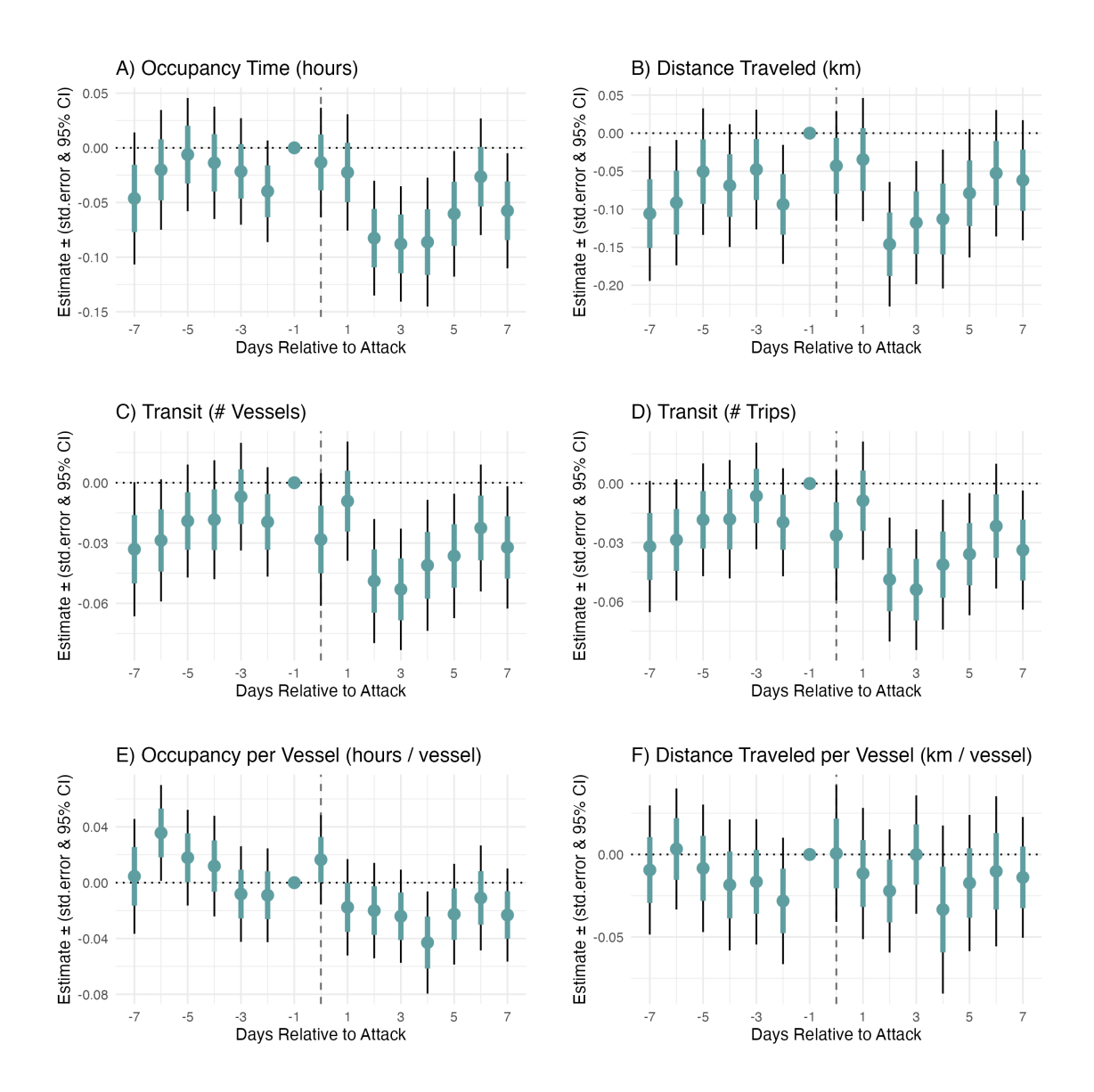


Figure 3: **Dynamic effects of piracy on ship transit.** The unit of observation is a grid cell-day (N=32,129). Each inset examines a different shipping activity measure. The horizontal axis shows time relative to the day of the attack. The vertical axis shows the magnitude of the effect. Points are coefficient estimates showing change in shipping activity. The thick colored portion of the error bars show Conley standard errors (50km cutoff), and the thin black portion shows 95% Confidence Intervals.

suggest a temporary reduction in traffic that resolves over a 7-day window. Following this insight, we investigate the relationship between reported pirate encounters and changes in voyage characteristics. The regression results are summarized in Table 1, with additional details in Supplementary Information B. We observe that a piracy encounter along a vessel's likely voyage path leads to longer average travel distances and prolonged travel times. The global estimate suggests that an additional pirate encounter (within the preceding 7 days and along a vessel's likely voyage path) translates to an extra 70 km in distance and 3 hrs in travel time. We observe consistent results when restricting the sample to voyages that traverse hotspots, although the effect is much more pronounced for voyages passing through the Gulf of Aden (300 km and 12 hr, respectively).

In contrast to the economically meaningfully impacts on travel distance and time, the effect on speed is minimal (if statistically significant). We interpret these results as an indication that adjustments to speed are less cost-effective as an avoidance measure, or technically inefficient or infeasible due to engine and vessel constraints. We also note that this behavior is consistent with optimal avoidance, since the cost of each additional unit of distance traveled grows linearly, while the cost per each additional unit of cruising speed grows exponentially [49]. These results are robust to specification, subsampling, and data construction decisions. Again, Supplementary Information D.2 provides full details.

2.3 The welfare costs of piracy

How much does all of this avoidance behavior cost in monetary terms? While operational costs are not directly observable to us, we can address this question by using vessel characteristics to determine the likely fuel and labor requirements along a given voyage. The results from this cost estimation exercise are available in Supplementary Information B. Summarizing, and consistent with our other findings, we estimate that a pirate encounter during the preceding 7 days translates to an average increase of about US\$2,500 in input costs per voyage (comprising US\$2,100 in fuel and US\$400 in labor). While this estimate remains largely consistent across data samples, again we observe a considerably larger effect in the Gulf of Aden. Our estimates for this hotspot suggest that an additional pirate encounter is associated with a per-voyage cost of roughly US\$13,600 (US\$12,000 in fuel plus US\$1,600 in labor).

Table 1: Effect of Past Pirate Encounters on Shipping Voyages.

	Global	G. of Aden	G. of Guinea	S.E. Asia				
Panel (A): Total Distance (km)								
Encounters (7 day)	64.91*** (6.64)	300.68*** (28.67)	58.07*** (3.15)	49.56*** (6.98)				
Panel (B): Total Time (hr)								
Encounters (7 day)	3.18*** (0.33)	12.18*** (1.18)	3.56*** (0.26)	2.47*** (0.35)				
Panel (C): Average Speed (km/hr)								
Encounters (7 day)	0.05*** (0.01)	0.37*** (0.04)	0.06** (0.03)	0.05*** (0.01)				
Observations	26,777,022	1,003,520	346,715	6,377,789				
Hotspot FE	_	\checkmark	\checkmark	✓				

^{*} p < 0.1, *** p < 0.05, *** p < 0.01. The unit of observation is a voyage. Each panel examines an observed feature in terms of total distance in kilometers (km), total time of the voyage in hours (hr), and the average speed of the voyage (km/hr). The sample spans from 2013 to 2021. Every column is a different sample: Global is the analysis using the whole sample. G. of Aden, S.E. Asia, and G. of Guinea restrict the sample to vessels passing through one of the hotspots, respectively. Every panel-column combination is a different regression analysis. Encounters (7 day) is the count of pirate encounters recorded in the projected path of the vessel in the preceding 7 days from the departure date using a 5 degree spatial footprint. Controls include average wind speed along the voyage, the wind-resistance index, and wave height. Fixed effects include country-to-country combination, vessel type, vessel size, hotspot, and a battery of month by year and top port-to-port combination for country-to-country combination dummies.

Increases in fuel consumption have an additional environmental and social impact due to the emissions of greenhouse gases and local pollutants that are harmful to human health. Here we focus on CO_2 , NO_x and SO_x emissions, since these pollutants are particularly relevant for the shipping industry. Detailed results by year and pollutant are provided in Supplementary Information B. Overall, we estimate that every additional pirate encounter leads to an approximate increase of 10 tons of CO_2 , 244 kg of NO_x , and 200 kg of SO_x per voyage, respectively. NO_x and SO_x excess emissions are relatively less voluminous, but this is to be expected given their smaller concentrations in bunker fuel relative to carbon. Once again, limiting the analysis to the Gulf of Aden suggests impacts that are an order of magnitude larger.

To contextualize the practical significance of these estimates, we contrast the implied operational and pollution costs of avoidance behavior during our full 2012–2023 sample with a counterfactual scenario that is absent any pirate activity. Figure 4 maps the average annual costs to the shipping industry (fuel and labor costs), and the additional emission of air pollutants. To monetize these impacts, we use the social cost of each pollutant [26, 34] and derive an aggregate measure of the global costs of piracy that averages US\$5.4 billion/year. This figure corresponds to about 1.95\% of the total private and public cost generated in our sample. Approximately US\$1.33 billion of this topline number is attributable to private operational (fuel and labor) costs, while US\$4.15 billion are attributable to public damages (due to climate change and local air pollution). ASAM regions 7 and 9 (containing the Southeast Asian hotspot) account for US\$2.59 billion and US\$1.44 billion, ASAM region 6 (containing the Gulf of Aden) accounts for US\$750 million, and ASAM region 5 (Gulf of Guinea) accounts for US\$623 million. The results underlying Figure 4 are reported in detail in Supplementary Information C. We note that NO_x and SO_x are pollutants that mostly affect the region where they are emitted, so we constrain the impacts of NO_x and SO_x emissions to each nation's Exclusive Economic Zone (200 nautical miles) or Contiguous Zone (24 nautical miles). We find that 87.45% of the total costs occur within Exclusive Economic Zones, and that 9.8% occur within the Contiguous Zones.

Adjustments by individual vessels may be small, but the high density of shipping transits in places where pirate encounters occur leads to substantial economic damages in the aggregate; particularly when public costs are accounted for.

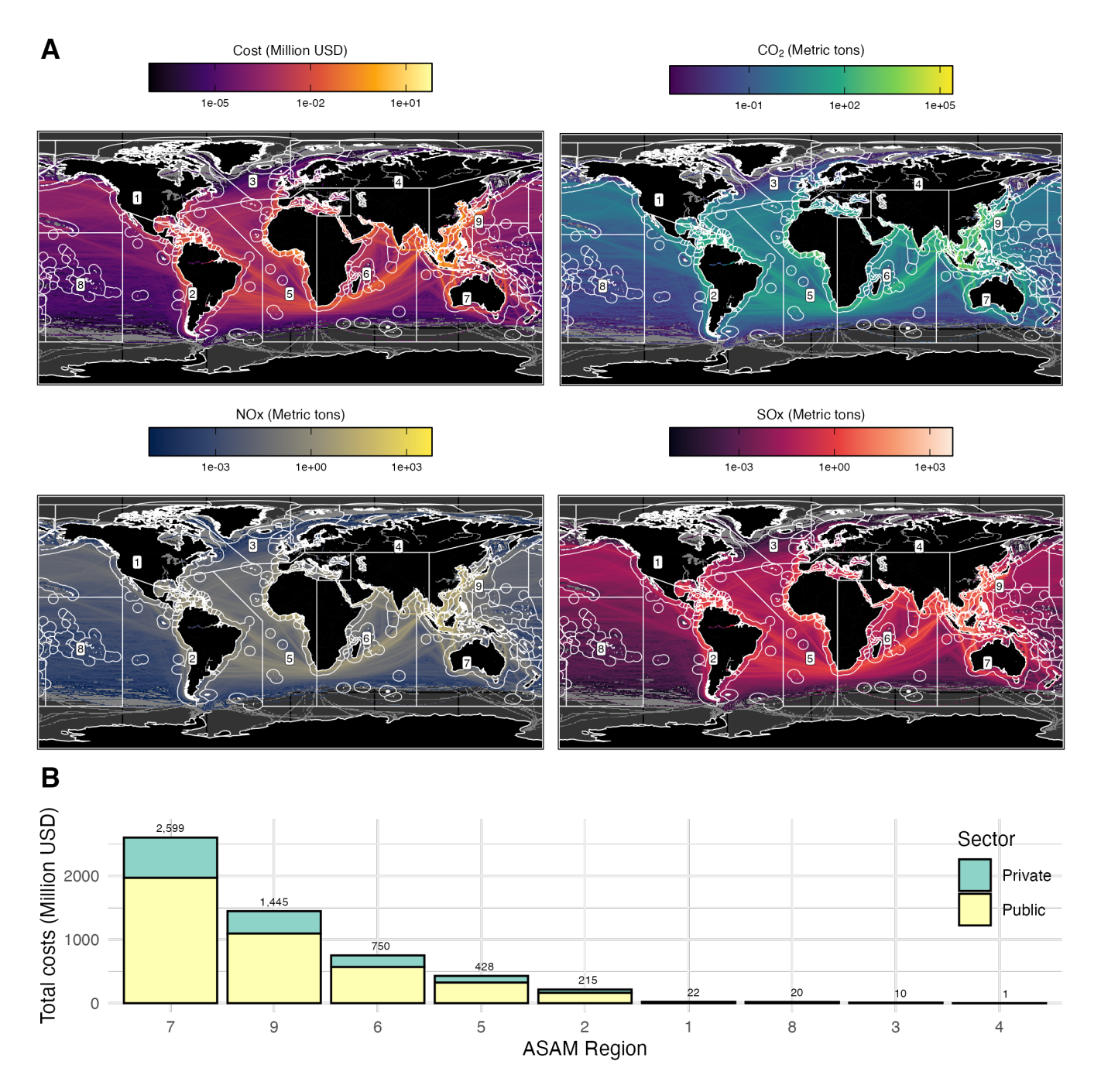


Figure 4: Additional Operational Costs and Emissions due to Piracy. Panel A shows maps of mean annual private costs to shippers (labor and fuel costs; Million USD), and additional CO_2 , NO_x , and SO_x emissions (Metric tons). Note that data are \log_{10} -transformed for visualization purposes and represented using a $0.5^{\circ} \times 0.5^{\circ}$ grid in geographic coordinates. Panel B shows the total costs (Million USD) associated with piracy by ASAM region, where we sum private costs to shippers as well as the cost of damages imposed by additional emissions based on the social-cost of each pollutant.

3 Discussion

This paper has examined the effect of piracy on the global shipping industry. First, we documented the avoidance behavior that shippers adopt in response to reported pirate encounters. Then we mapped these responses to individual adjustments along a route, before deriving the implied aggregate welfare effects (comprising both private costs and public environmental damages). While our estimated adjustment costs may seem relatively small at the individual level, cumulatively they translate to a significant economic welfare loss in the aggregate. Taking the total flow of global shipping routes into account, together with the prevalence of pirate encounters in some of the world's busiest shipping channels, we find that piracy avoidance is a considerable cost to the shipping industry. Moreover, it is an overlooked but material source of environmental externalities.

The simple economic intuition underlying our analysis suggests that ships adjust their voyages to reduce the probability of pirate encounters. But those adjustments do not necessarily mean a complete change of routes (i.e., start and end ports remain the same). This intuition holds up well in the data, where we observe short-lived regional avoidance behavior, which is related to ships traversing longer paths along a port-to-port route, at the cost of higher fuel consumption and labor time. Each additional encounter amplifies this behavioral response, and the effects have long-term implications after a single encounter is reported.

As we have tried to emphasize, the Gulf of Aden is something of an outlier in our empirical results. The effects that we observe here are an order of magnitude larger than elsewhere, even other piracy hotspots. Why would the Gulf of Aden present such a different level of adjustment? One possibility is salience and the prominence that these assaults, particularly from Somali pirates, have gained in the public perception. But it could also reflect the geographical characteristics of the region, which allows for a more diverse set of adaptive actions for a given route. For example, vessels traveling between Europe and Asia can decide between traversing the Gulf of Aden and crossing through the Suez Canal, or circling around the Cape of Good Hope. By contrast, all vessels destined for Nigeria must traverse the Gulf of Guinea hotspot. The way in which captains assess the relative piracy risk along a given path, and the potential cost of doing so in different regions, affects the scope of their adaptation.

Such regional heterogeneity notwithstanding, we emphasize that the effect of piracy is clear

and consistent across space and when measured at the voyage level. The consistency of the results from two different empirical approaches highlights that piracy is a global problem for the maritime shipping industry. However, it also underscores the potential for piracy to have wider impacts that ripple across the global economy. We can posit several channels through which these wider impacts manifest. The first is a simple waste of capital. Because individual shippers implement avoidance measures, they must allocate capital to cover these actions. Such capital could have been used somewhere else, either in the form of additional voyages, or as an input to other productive activities.

A second channel is through environmental impacts. The adjustments to piracy are not emission-neutral. In the aggregate, maritime commerce remains a significant source of pollutant emissions, with direct contributions to both global greenhouse emissions and local air pollutants that may disproportionately affect different areas and populations [15].

A third channel for wider economic impacts is the potential for indirect trade costs. Depending on the level of competitiveness of the affected industry, and the routes in question, the associated costs in transportation could simultaneously affect both producers and consumers. Previous studies have tried to explore this problem using a trade framework [8, 12], and we believe that our approach of examining individual voyages helps further clarify some of the mechanisms behind previously identified trade effects, both at a local and a global scale.

Stepping back, three key insights derive from our results. First, the piracy problem remains prevalent at a global scale. Second, the sheer density of shipping voyages, particularly in piracy hotspots, means that individual avoidance behaviors accumulate into economically meaningful costs in the aggregate. These losses not only reflect the direct impact on trade flows and transportation inputs, but also the indirect environmental and social costs from pollution. Third, our results highlight the potential value of enforcement and anti-piracy measures for piracy-prone areas. According to available public data [43], a cost-effective defense force could be deployed for roughly US\$330M/year, adjusted for inflation. Enforcement spending would thus cost a fraction of the total US\$1–4B value that we estimate is currently being lost due to piracy. Addressing this missing enforcement will require coordination and active cooperation from multiple sectors and nations. The benefits, however, could be enjoyed widely. Alternatively, funding could be deployed to alleviate poverty, thereby tackling the roots of the piracy

problem in the developing world. Poverty reduction partnerships, involving both public and private participation, could potentially prove highly cost-effective at reducing piracy risk. The design, implementation, and analysis of such policies is a promising area for future research.

4 Materials and Methods

4.1 Data

We construct two unique datasets for global shipping and piracy that provide both temporal and spatial variation. Specifically, we compile two panel datasets from 2012 to 2023 that include shipping vessel activity as well as pirate encounters: a voyage-level dataset, and a spatially gridded and aggregated 0.5°x0.5 dataset. Each panel covers all global valid cargo and tanker voyages between 2012 and 2023. For the voyage-level dataset, each voyage entry includes reporting vessel characteristics (type, size, crew), departure and arrival dates, departure and arrival ports and countries, total distance traveled (km), time traveled (hr), speed (km/hr), fuel consumption (kg), fuel and labor cost (US\$), and emissions of CO₂, NO_x, and SO_x (kg).

4.1.1 Shipping activity

Individual shipping vessel activity data come from Global Fishing Watch (GFW), which provides Automatic Identification System (AIS) data that is composed of high-resolution timestamped latitude and longitude messages which are received through satellite, terrestrial, and dynamic receivers [30]. We used the latest version of the GFW data processing pipeline, Version 3 [1], which builds on the original AIS data processing methods from [30] and expands coverage from fishing vessels to all types of vessels that carry AIS (including cargo and tanker vessels). AIS transponders are required on all vessels greater than 300 gross registered tons while operating on international voyages, and by many countries while operating in certain exclusive economic zones [33]. The dataset from 2012-2023 includes over 114,000 unique known cargo, tanker, and reefer types as defined by vessel identification data provided by GFW. We use the GFW vessel classification algorithm, which leverages publicly-available registry information where available and machine learning algorithms where not available, to include only those vessels that are classified by GFW as one of cargo, cargo or tanker, bunker or tanker,

tanker, cargo or reefer, specialized reefer, container reefer, reefer, or bunker.

These vessels broadcast more than 16 billion individual AIS messages during our study period, which we aggregate into our voyage-level and gridded datasets. For the voyage-level dataset, we leverage GFW's datasets of ports and voyages in order to assign every single AIS message to a specific port-to-port voyage by a specific vessel [51]. Out of 33 million possible voyages, we restrict our analysis to those approximately 26.7 million voyages that meet the following criteria: 1) have full weather information; 2) the vessel has a realistic design speed greater than 10 knots (see below); 3) it is not missing information on the departure or arrival countries; and 4) it does not pass through multiple hotspots.

For the gridded version of the dataset, we calculate the daily occupancy time (hours), distance traveled (km), number of vessels, and number of trips that transit through pixels with at least one pirate encounter during our study period. For both the voyage-level and gridded versions of the dataset, we filter the data to only include shipping activity from trips with reliable profiles: we only include trips that have total distance traveled and hours spent each greater than zero; we only include trips that are less than or equal to 60 days; we only include trips with a total distance traveled less than or equal to the earth's circumference (40,075 km); and we only include trips with a total distance traveled less than or equal to four-times the average observed distance for each port-to-port route.

4.1.2 Shipping operational costs

For our voyage-level dataset, we calculate operational costs from two sources: fuel consumption and labor. We calculate fuel consumption using main engine power, gross tonnage, auxiliary engine power, and design speed. Main engine power and gross tonnage come from the Global Fishing Watch vessel characteristics database [30]. For each vessel, we determine these characteristics using a hierarchy based on data availability: 1) the official registered information of the vessel; and 2) values inferred by the Global Fishing Watch vessel characteristic neural network when available. Auxiliary power is a function of main engine power, and is calculated using known empirical relationships [9], which link main propulsory requirements with vessel characteristics and auxiliary needs. Design speed is a function of main engine power and gross tonnage based on the regression results from [9]. Since this regression can sometimes lead to

abnormally low design speed values, we limit our voyage-level analysis to only those vessels for which we calculate an estimated design speed above 10 knots.

Using these vessel characteristics, we calculate fuel consumption using a standard approach that combines fuel consumed by both the main and auxiliary engines [16]. Fuel consumption of the main engine is defined by hours of operation, main engine power, main engine specific fuel consumption rates [48], and a cubic law of operational speed relative to design speed. Fuel consumption of the auxiliary engine is defined by operating hours, auxiliary engine power, and auxiliary engine specific fuel consumption rates [48]. Fuel consumption was calculated for each individual AIS ping, which was then summed across pings for each voyage. We are missing engine power data from 2,816 vessels, meaning that we cannot calculate fuel consumption, fuel cost, or emissions for voyages by these vessels.

Daily fuel price data come from Bunker Index. We use the 380 CST Bunker Index, which is the global average price from all ports selling 380 centistoke fuel, the most commonly used fuel in maritime transport. Although there is some spatial variation in bunker fuel price across different ports, these regional price data are not publicly available. Our fuel price time series runs from January 1, 2012 through October 19, 2023, meaning that trips starting after October 19, 2023 will have missing fuel cost information. For dates with missing price data within this time range, we impute the missing value using the most recent reported price. Most gaps in the data do not exceed more than two days. Total fuel cost for each voyage is then calculated by multiplying the total fuel consumption of the voyage by the fuel price on the date of departure.

We also keep track of labor requirements and costs for individual voyages. Using the ratio suggested in the literature [9], we estimate the crew needed to operate a vessel as a function of its size and type. The crew wage is calculated using the 2018 International Transport Worker's Federation wage scale for the average non-officer seafarer [27].

4.1.3 Emissions

We also calculate emissions of CO_2 , NO_x , and SO_x for each voyage. CO_2 emissions are calculated using a linear relationship [16], which relies on total fuel consumption of the voyage. SO_x emissions are calculated similarly, under the assumption of 3.3% sulfur content for each kilogram of fuel [15]. Similarly, NO_x emissions are calculated using a separate conversion rate

for both the main engine fuel consumption (which we assume to be a slow-speed engine) and auxiliary engine (which we assume to be a medium-speed engine) [15].

4.1.4 Weather proxies

Finally, for the voyage-level dataset, we incorporate weather proxies in the forms of average wind speed and direction along each voyage (which we call the wind-resistance index), as well as average surface wave height (which is the combined significant height of both wind waves and swell). Both wind and wave height data come from the Copernicus ERA5 reanalysis model [24]. We download monthly data provided at 0.25×0.25 degree resolution. Mean monthly wind speed, wind direction, and surface wave height information is calculated for $5^{\circ} \times 5^{\circ}$ grid cells. For wind speed and wind direction we use a vector averaging approach, in which we first take the individual averages of the u and v vectors of wind speed, and then use those averaged u and v vectors to calculate the average vector wind speed and direction [20]. We take into account wind direction by decomposing the pitch angle relative to the heading of the vessel; the resistance is concave or convex depending on the vessel going against, or with the wind. This measurement is symmetric in absolute terms along each 90° portion of a full circumference and it goes from 0 to 1. Scaling this measurement by the wind speed gives the final wind-resistance index. For each voyage, we calculate the mean wind-resistance and mean surface weight height from across the $5^{\circ} \times 5^{\circ}$ pixels that the voyage passed through.

4.1.5 Pirate encounters

We operationalize pirate encounters by using data provided by the United States National Geospatial Intelligence Agency, which includes dates and locations of sightings and hostile acts against ships by pirates, robbers, and other aggressors [35]. To construct a dataset of encounters that we believe would influence shipping behavior, we manually examined the written description of all encounters between 2012 and 2023, and removed those that occurred in or near ports, inland waterways, were associated with military operations, were not actually aggressive or violent, or could not actually be confirmed. Each description of an encounter was reviewed by two independent readers. Any descriptions with disagreements were reviewed a third time to reach a 2/3 consensus. This resulted in a final dataset of 2,611 encounters that

occurred from 2012-2023.

We then divide the ocean into two global grids: one of 0.5° latitude by 0.5° longitude pixels and one of 5° latitude by 5° longitude pixels. We use the $0.5^{\circ} \times 0.5^{\circ}$ data for a fine-scale pixel-level analysis, and use the $5^{\circ}x5^{\circ}$ data for a port-to-port voyage-level analysis.³ For each gridded dataset, we then calculate the number of encounters that occurred in each pixel on each day. For any given pixel and any given day of shipping operation in that pixel, this therefore allows us to calculate the number of days since the most recent encounter in that pixel, as well as the number of encounters that occurred within that pixel over a rolling time window. For the pixel-level analysis, we build an indicator variable indicating whether grid cell i in day t had a reported pirate encounter.

For the voyage-level analysis, we calculate a suite of encounter indicators. Each of these provides an indication for the number of recent pirate encounters in the area that each voyage passes through. These represent, for any given voyage departure date for any given port-to-port route, the captain's set of information on piracy risk along the route they are about to embark on. For each voyage, we first calculate the number of unique previous encounters within the exact set of 5°x5° pixels that the vessel itself transited through. We do so by aggregating previous unique encounters across rolling windows of the 7, 15, and 30 days prior to the voyage start. This allows us to examine how different lags for aggregating previous unique encounters affect shipping behavior. Next, we calculate the number of days since the most recent encounter that occurred anywhere along the pixels each voyage transited through.

For robustness checks on the grid-level analysis, we repeat the process but this time using a higher spatial resolution of 0.1°x0.1° and a coarser grid of 1°x1°. See Supplementary Information D). For the voyage-level analysis, we also calculate the *average* number of unique encounters that occurred along *previous* voyages for each port-to-port route, by voyage, over the rolling time windows. We calculate each of these indicators by either aggregating previous unique encounters for the 3°x3° or the 7°x7° pixels each previous voyage passed through. Finally, we calculate the *total* number of unique encounters that occurred along all previous voyages that occurred along each port-to-port route, by trip, over rolling time windows of 7.

³At the equator, a cell of 5° by 5° is roughly equivalent 345 by 345 miles, which is a reasonable spatial area over which shipping vessel operators might make route and speed adjustment decisions in relation to recent piracy encounters. Moving at 10 knots, this is an area that potential attackers could cover in just 30 hours.

15, and 30 days. We again calculate each of these indicators by either aggregating previous unique encounters for the 5°x5° pixels each previous voyage passed through, or by the 3°x3° pixels each previous voyage passed through.

Using the locations of individual pirate encounters that occurred from 2012 through 2023, we also determine hotspots of encounters using density-based clustering as described by [17]. Implementing a cluster reachability distance of 10, and a minimum number of encounters per cluster of 150, we find three hotspots of intensive pirate activity for the entire panel: the Gulf of Aden, the Gulf of Guinea, and Southeast Asia. For each of these hotspots, we generate a rectangular bounding box that is snapped to the nearest 5° latitude and 5° longitude markers that fully enclose each set of hotspot encounters. For the pixel-level $0.5^{\circ} \times 0.5^{\circ}$ gridded analysis, we then determine which (if any) hotspot each pixel falls within. For the voyage-level dataset, we determine which (if any) hotspots each shipping vessel transited through during each voyage.

The final overlap between shipping voyages and pirate encounters, which is the dataset used in the voyage-level empirical analysis, is shown in Figure 1. Note that pirate encounters concentrate in a few areas in the map. Particularly in the Gulf of Guinea, the coast of East Africa, the Arabian Sea, and the jurisdictional waters of the Philippines and Malaysia. The relevant hotspots for this study are enclosed by the rectangles.

4.2 Empirical analysis

4.2.1 Grid-level analysis

To establish the effect of piracy on shipping we will rely on several estimation procedures. First, we begin by generally asking if shipping transit is apparently affected by pirate encounters. The analysis is performed under an Eulerian framework, with the units of analysis as grid cells along a $0.5^{\circ} \times 0.5^{\circ}$ grid. In particular, we are interested in how measures of shipping traffic (i.e., occupancy time, total distance traveled within a grid cell, number of voyages and vessels crossing a grid cell) change following a pirate encounter. Summary statistics for these data are provided in Table B.1.

We implement this analysis using an event study design to examine the dynamic response of shipping traffic to pirate encounters. We estimate the following regression model for grid cell i at time t:

$$y_{it} = \sum_{k=-7, k \neq -1}^{7} \beta_k D_{it}^k + \eta_i + X_t + \omega_t + \epsilon_{it}$$
 (1)

Here, y_{it} is the outcome of interest in grid cell i at time t, and has been inverse-hyperbolic-sine-transformed. The key variables of interest are a set of event-time dummy variables, D_{it}^k . Each dummy D_{it}^k equals one if grid i at time t is k days relative to a pirate event (e.g., k = -7 is 7 days prior, k = 7 is 7 days after). A pirate event is a cluster of pirate encounters that occur within a 7-day window.

 β_k captures the average marginal change in traffic k days before or after a pirate event, relative to the omitted baseline period one day before the event. The model includes grid cell-specific fixed effects (η_i) , which absorb all time-invariant differences across cells, year-by-month fixed effects (X_t) to capture flexible temporal trends, and day-of-week fixed effects (ω_t) to account for weekly cycles in economic activity. We estimate Conley standard errors with a 50 km cutoff [14]. This analysis restricts the sample to grid cells with at least one encounter during our analysis window (2012-2023; N = 618 grid cells and 32,139 observations). The identification assumption is that the timing of an encounter is exogenous to contemporaneous shocks in shipping traffic, after controlling for the comprehensive set of grid and time fixed effects.

4.2.2 Voyage-level analysis

We then analyze the effect of piracy at the voyage level. We are interested in the feature of a given voyage i (i.e., distance, duration, and speed) along country-to-country route, r, at time t, and their associated consequences in terms of operational costs and emissions. The model is as follows:

$$y_{irt} = \alpha + \beta T N E_{rt} + \delta_i V C_i + \lambda_i W_i + \eta_r R_i + \theta' X_t + \epsilon_{irt}$$
 (2)

y is the response variable, and TNE is the total number of encounters during the last seven days, with β as the average marginal effect of an additional encounter on the mean path of a voyage. VC is a vector of fixed effects according to vessel characteristics (i.e., type of vessel

and size), while W is the time-weighted mean wind-resistance index, average wind speed, and average wave height for a given voyage. Finally, R is a vector of fixed effects by route, while X_t is a battery of month by year fixed effects. In the results we will also specifically control for additional factors such as crossing hotspots or the voyage being part of the most common port-to-port combination between countries. To account for potential route and temporal correlation, we cluster standard errors by country-to-country route by year. The identification assumption is that the timing and location of past encounters are exogenous to the date of departure of a given vessel.

Acknowledgements

We thank Christopher Costello, Anca Cristea, Javier Birchenall, Kyle Meng, Olivier Deschenes, Owen Liu, and Christopher Severen for helpful comments on the paper. We also acknowledge valuable feedback from participants at the Econometrics Lunch and the Environmental Lunch at the University of California at Santa Barbara (UCSB), the Workshop in Environmental Economics and Data Science at the University of Oregon, and the Summer Conference of the Association of Environmental and Resource Economics. We thank Global Fishing Watch for providing the data processing and data management infrastructure for the shipping data. We would also like to thank Google for providing in-kind computational support.

Funding

Partial funding for this project was provided by the Research Provost Award at the University of Miami, the Latin American Fisheries Fellowship at the University of California Santa Barbara, the Chilean Government through the Becas Chile program, and the Environmental Markets Laboratory at the University of California, Santa Barbara.

Author Contribution

Conceptualization was performed by R.M, J.C.V.D., G.McDo., and G.McDe. Data curation was performed by R.M, J.C.V.D., and G.McDo. Formal Analysis was performed by R.M and J.C.V.D. Funding acquisition was performed by R.M. Investigation was performed by

R.M, J.C.V.D., and G.McDo. Methodology was performed by R.M, J.C.V.D., G.McDo., and G.McDe. Project administration was performed by R.M. Supervision was performed by R.M. Validation was performed by R.M, J.C.V.D., G.McDo., and G.McDe. Visualization was performed by R.M., J.C.V.D. and G.McDo. Writing – original draft was written by B.M., J.C.V.D., G.McDo., G.McDo., G.McDo., G.McDo. Writing – review & editing was performed by R.M., J.C.V.D., G.McDo., and G.McDe.

Competing interests

441

442

443

444

445

446

447

448

450

451

The authors declare no competing interests.

Data and materials availability

All data and materials will be available at https://github.com/renatomolinah/piracy-shipping

References

- [1] 2024 Aug New release in our AIS data pipeline (version 3). Accessed: 2025-07-21.

 2024. URL: https://globalfishingwatch.org/faqs/2024-aug-new-release-in-our-ais-data-pipeline-version-3/.
- John L Anderson. "Piracy and world history: An economic perspective on maritime predation". In: *Journal of World History* (1995), pp. 175–199.
- 457 [3] Kenneth R Andrews. *The Spanish Caribbean: trade and plunder, 1530-1630.* Yale
 458 University Press New Haven, 1978.
- Regina Asariotis et al. Review of Maritime Transport, 2017. Tech. rep. United
 Nations Conference on Trade and Development, 2017.
- [5] Sebastian Axbard. "Income opportunities and sea piracy in Indonesia: Evidence from satellite data". In: *American Economic Journal: Applied Economics* 8.2 (2016), pp. 154–94.

- Jay Bahadur. "Deadly waters. Inside the hidden world of Somalia's pirates". In:

 US Naval Institute Proceedings. Vol. 137. 8. 2011, pp. 73–74.
- Jay Bahadur. The pirates of Somalia: Inside their hidden world. Vintage, 2011.
- Sami Bensassi and Inmaculada Martinez-Zarzoso. "How costly is modern maritime piracy to the international community?" In: Review of International Economics 20.5 (2012), pp. 869–883.
- [9] Sarah Betz. "Reducing The Risk of Vessel Strikes to Endangered Whales in the Santa Barbara Channel". PhD thesis. University of California, Santa Barbara, 2011.
- 473 [10] Anna Bowden et al. *The economic costs of maritime piracy*. One Earth Future Foundation, 2010.
- Christian Bueger. "Practice, pirates and coast guards: The grand narrative of Somali piracy". In: *Third World Quarterly* 34.10 (2013), pp. 1811–1827.
- 477 [12] Alfredo Burlando, Anca D Cristea, and Logan M Lee. "The trade consequences of maritime insecurity: evidence from Somali piracy". In: *Review of International*479 *Economics* 23.3 (2015), pp. 525–557.
- [13] CNN. Piracy threat returns to African waters. 2023. URL: https://t.ly/qKlZo (visited on 11/06/2025).
- Timothy G Conley. "GMM estimation with cross sectional dependence". In: *Journal of econometrics* 92.1 (1999), pp. 1–45.
- ⁴⁸⁴ [15] James J Corbett and Paul Fischbeck. "Emissions from ships". In: *Science* 278.5339 (1997), pp. 823–824.
- James J Corbett, Haifeng Wang, and James J Winebrake. "The effectiveness and costs of speed reductions on emissions from international shipping". In: *Trans-*portation Research Part D: Transport and Environment 14.8 (2009), pp. 593–598.
- Martin Ester et al. "A density-based algorithm for discovering clusters in large spatial databases with noise." In: *Kdd.* Vol. 96. 34. 1996, pp. 226–231.

- [18] Matthias Flückiger and Markus Ludwig. "Economic shocks in the fisheries sector and maritime piracy". In: *Journal of Development Economics* 114 (2015), pp. 107–125.
- Philip Gosse. The history of piracy. Courier Corporation, 2012.
- [20] SK Grange. "Technical note: Averaging wind speeds and directions. 2014". In:

 View Article ().
- [21] Todd Gray. "Turkish piracy and early Stuart Devon". In: Reports of the Transactions of the Devonshire Association for the Advancement of Science 121 (1989), p. 161.
- 500 [22] Brishti Guha and Ashok S Guha. "Pirates and traders: Some economics of pirate-501 infested seas". In: *Economics letters* 111.2 (2011), pp. 147–150.
- Paul Hallwood and Thomas J Miceli. "An economic analysis of maritime piracy and its control". In: Scottish Journal of Political Economy 60.4 (2013), pp. 343–359.
- Hans Hersbach et al. "The ERA5 global reanalysis". In: Quarterly journal of the royal meteorological society 146.730 (2020), pp. 1999–2049.
- [25] ICC-IMB. Piracy and Armed robbery Against Ships: Report for the Period 1 January - 31 December 2017. Tech. rep. International Maritime Bureau of the International Chamber of Commerce, 2018.

510

511

512

516

517

- [26] Interagency Working Group on Social Cost of Greenhouse Gases [United States Government]. Technical support document: Social cost of carbon, methane, and nitrous oxide interim estimates under executive order 13990. Online. Feb. 2021.
- International Transport Workers' Federation. ITF Seafarers Wages and compensation. Accessed: 2025-11-06. 2025. URL: https://www.itfseafarers.org/en/resources/wages (visited on 11/06/2025).
 - [28] Ali Kamal-Deen. "The anatomy of Gulf of Guinea piracy". In: Naval War College Review 68.1 (2015), pp. 93–118.

- Amarilla Kiss. "Maritime Piracy in the Modern Era in Latin America: Discrepan-|29|518 cies in the Regulation". In: Acta Hispanica II (2020), pp. 121–128. 519
- David A Kroodsma et al. "Tracking the global footprint of fisheries". In: Science [30]520 359.6378 (2018), pp. 904–908. 521
- Peter T Leeson. "An-arrgh-chy: The law and economics of pirate organization". [31]522 In: Journal of political economy 115.6 (2007), pp. 1049–1094. 523
- [32]Carolin Liss. "Privatization of maritime security in Southeast Asia". In: Private 524 Military and Security Companies. Springer, 2007, pp. 135–148. 525
- [33]Douglas J McCauley et al. "Ending hide and seek at sea". In: Science 351.6278 526 (2016), pp. 1148–1150. 527

528

529

530

531

532

541

- Mathias Mier, Jacqueline Adelowo, and Christoph Weissbart. "Taxation of Carbon |34|Emissions and Local Air Pollution in Intertemporal Optimization Frameworks with Social and Private Discount Rates". Online. Dec. 2021. URL: https://www. ifo.de/DocDL/wp-2021-360-mier-adelowo-weissbart-social-cost-airpollution-carbon.pdf.
- National Geospatial-Intelligence Agency. Anti-Shipping Activity Messages (ASAM) |35|533 database. 2024. URL: https://msi.nga.mil/Piracy (visited on 11/06/2025). 534
- National Geospatial-Intelligence Agency. Worldwide Threats to Shipping Report, |36|535 04 Jul 2013. Accessed: 2025-11-06. 2013. URL: https://msi.nga.mil/api/ 536 publications/download?key=16920958/SFH00000/wwtts_20130704100000. 537 txt (visited on 11/06/2025). 538
- Ryan J O'Connell and Christopher M Descovich. Decreasing variance in response [37]539 time to singular incidents of piracy in the Horn of Africa area of operation. Tech. 540 rep. Naval Postgraduate School Monterey CA Department of Information Sciences, 2010. 542
- [38]Office of Naval Intelligence. Worldwide Threats to Shipping (WWTS) Reports. 543 Accessed: 2025-11-06. 2025. URL: https://t.ly/frrm6 (visited on 11/06/2025). 544

- International Martime Organization. Guidelines for the onboard operational use of

 shipborne AIS: Resolution A.917(22). Accessed: 2025-11-07. 2001. URL: https://

 www.cdn.imo.org/localresources/en/KnowledgeCentre/IndexofIMOResolutions/

 AssemblyDocuments/A.917(22).pdf (visited on 11/07/2025).
- [40] George Ad Psarros et al. "On the success rates of maritime piracy attacks". In:

 Journal of transportation security 4.4 (2011), p. 309.
- [41] Alfred P Rubin. "Law of Piracy, The". In: Int'l L. Stud. Ser. US Naval War Col.
 63 (1988), p. 13.
- Geoffrey Vaughn Scammell. "European exiles, renegades and outlaws and the maritime economy of Asia c. 1500–1750". In: *Modern Asian Studies* 26.4 (1992), pp. 641–661.
- Dirk C Sonnenberg. "Maritime Law Enforcement A Critical Capability for the Navy". PhD thesis. Monterey, California. Naval Postgraduate School, 2012.
- 558 [44] Alberto Tenenti. Piracy and the Decline of Venice, 1580-1615. Univ of California 559 Press, 1967.
- The Wire. Abduction of Crew Off Nigeria Brings Piracy Back to Indian Agenda.

 2023. URL: https://t.ly/gVVXJ (visited on 11/06/2025).
- 562 [46] Time. Pirates in Southeast Asia: The World's Most Dangerous Waters. 2023. URL:
 563 https://t.ly/Ano8q (visited on 11/06/2025).
- United Nations. Report of the Secretary-General on the situation in Haiti. 2024.

 URL: https://rb.gy/6rku6u (visited on 11/06/2025).
- Chengfeng Wang, James J Corbett, and Jeremy Firestone. "Modeling energy use and emissions from North American shipping: application of the ship traffic, energy, and environment model". In: *Environmental science & Eamp*; technology 41.9 (2007), pp. 3226–3232.

- 570 [49] Shuaian Wang and Qiang Meng. "Sailing speed optimization for container ships 571 in a liner shipping network". In: *Transportation Research Part E: Logistics and* 572 *Transportation Review* 48.3 (2012), pp. 701–714.
- [50] James Francis Warren. The Sulu Zone, 1768-1898: The dynamics of external trade, slavery, and ethnicity in the transformation of a Southeast Asian maritime state. NUS Press, 2007.
- 576 [51] Global Fishing Watch. Anchorages, ports and voyages data. June 2021. URL: https://globalfishingwatch.org/datasets-and-code-anchorages/.
- 578 [52] Heather Welch et al. "Hot spots of unseen fishing vessels". en. In: Sci. Adv. 8 (44 579 Nov. 4, 2022), eabq2109.
- 580 [53] R Wright. "Piracy set to escalate shipping costs". In: Financial Times, November 20 (2008).

82	Supplementary Information for:					
83	Dangerous Waters: The Economic Toll of Piracy					
84	$on \ Maritime \ Shipping$					
85	Renato Molina, Juan Carlos Villaseñor-Derbez,					

Gavin McDonald & Grant McDermott

A Background

A.1 Piracy and trade

Modern piracy is fundamentally an enforcement problem that can be traced to poorly defined property rights and duties over maritime territory. This misalignment is especially acute in international settings, where the establishment and enforcement of anti-pirate regulations usually conflicts with sovereign rights [41]. These institutional settings reduce the probability of pirates being prosecuted, or even apprehended, which in equilibrium encourages the continued predation of sea commerce.

From a welfare perspective, Anderson suggests several types of losses associated with piracy [2]. First, the direct capital losses to violence, which manifest either in the form of damages to the ship or cargo, or as the loss of life. Second, the indirect losses in the form of resources channeled toward evasion and protection that could have been used for other productive activities. For example, the additional bulk of fuel used to maintain evasive maneuvers, or the additional amount of capital required to sustain a steady flow of goods *vis-á-vis* the same exchanges in the absence of piracy. It follows that the magnitude of these responses can lead to both intensive and extensive margin adjustments, which in turn can cause dynamic losses in the form of diminished incentives for producers and merchants to continue with or expand production [2].

Historical data suggest that piracy events have often been followed by extremely negative impacts to commerce channels and local economies. For example, during the seventeenth century, the "Turkish pirates" completely paralyzed several parts of west England [21]. During the same period, the predominance of pirate organizations in the Arabian sea also led to severe decreases in trade flow, with devastating consequences for all industries in the region [42]. These two cases are not unique. Similar links have been documented for other trade regions in the Caribbean [3], the Philippines [50], and Venice [44]. All of these examples illustrate how thriving economies suffer considerable negative effects due to piracy.

Modern piracy has had similar effects. In fact, piracy remains a problem worldwide. There were over 2,600 pirate encounters globally between 2012-2023, with over 600 taking place between 2019-2023. Most encounters, however, take place in a few hotspots; namely: the Gulf

of Aden (known for the Somali pirates), the Gulf of Guinea (mostly within the Nigerian EEZ), the Malacca Straits (the shipping channel formed by Sumatra and the Malay peninsula) and the South China sea. For the remainder of the paper we will refer to both the Malacca Straits and the South China sea as one group that we call Southeast Asia. The distribution of the actual number of encounters in each region over time is shown in Figure 1. From this figure, note that pirate encounters are consistently concentrated in the African region and Southeast Asia.

Although sparse, there are several assessments regarding the economic impact of modern piracy. Past estimates suggest that the losses in trade volume due to pirate activities in Somalia accrued to about \$24 billion/year [12]. Other estimates are more conservative and suggest that the loss ranged between \$1 billion and \$16 billion, when accounting for the addition of 20 days per voyage due to re-routing around Africa, and increased insurance, charter rates, and inventory costs [53, 10, 37]. Another study estimates that 10 additional hijacks in either the Gulf of Aden or the Strait of Malacca reduce the volume of exports between Asia and Europe by about 11%, with an estimated cost of about \$25 billion per year [8]. These studies estimate losses through the examination of overall trade patterns, but to the best of our knowledge, there is no study focusing on the behavior of individual shipping vessels. We believe the latter is a more direct way to disentangle the cost of piracy. It is plausible that the gap in the literature regarding the effect of piracy on shipping patterns is due to the difficulty of obtaining data on individual shipping voyages, but also because of the sparse data on pirate activities. Both of these issues are accounted for in this paper.

On the other hand, theoretical insights regarding the piracy problem can be traced to two studies. Namely, Guha and Guha [22], who model optimal patrolling and penalties under the option of self insurance, and Hallwood and Miceli [23], who explore optimal patrolling and penalties taking into account strategic interactions between pirates and shippers. Although very valuable contributions in terms of formalizing the theory behind pirate behavior, neither paper explored vessel adjustments along shipping routes as they focus on penalties and enforcement.

Other related literature has devoted efforts to several topics on both past and modern piracy. One of those topics relate to anti-piracy efforts. Anderson [2] documents the historical evolution of state and individual actions to control for piracy along shipping routes. Similarly, Liss [32] describes how modern piracy incentivizes shippers to employ private military companies or acquire their own defense mechanisms. Other empirical settings, including Flückiger and Ludwig [18], as well as Axbard [5], study how poor fishing conditions lead to an increase in pirate activity in Africa and Indonesia, respectively.

Finally, other authors such as Leeson [31] and Psarros, Christiansen, and Skjong[40] study the factors that contribute to pirates being more or less effective in terms of finding vessels, as well as extracting the most value out of these encounters. In addition and specific to the Somali case, O'Connell and Descovich [37] and Bahadur [6] document the social and economic institutions associated with pirate activities by identifying ransom procedures, operational supply chains, and community support.

A.2 The business model of modern piracy

Establishing how pirates operate globally presents several challenges. First, pirates often have little or no incentive to make the details of their operations known to the public. Nonetheless, there are still a few credible sources that allow us to establish the mechanics behind pirate encounters, and more importantly, use them as means for identification in the empirical section. In particular, we make use of the information documented by Bahadur [7], which relies on a number of interviews with individuals who claimed to be associated, directly or indirectly, with pirates in Somalia in 2009. Considering the sensitivity of the piracy issue, these interviews provide the best available information on the actual behavior and incentives of pirates.

Pirates in Somalia appear to not discriminate between vessels. Instead they opportunistically hijack vulnerable vessels that cross their path. Once the potential target is identified, pirates pursue the vessel until eventually capturing it, or the vessel is realistically out of reach. Neither the search or the pursuit are constrained by the jurisdictional boundaries of Somalia. The boarding strategy entails the pirate crew splitting into several skiffs, which approach the target vessel from all sides while waving and firing their weapons to scare the ship's crew. If the vessel stops, or the skiffs are able to keep up with it, the pirates would toss rope ladders onto the deck and then proceed to boarding. According to the accounts, crews rarely resist boarding once the pirates successfully get on the deck. The average reported success rate of

the pirates used to be about 20 to 30% [7].

Once the pirates successfully take control of the ship, they steer the vessel to a friendly port. At this location, an additional set of guards and translators would board the ship, and ransom negotiations will start. Most ransoms would be handled by insurance companies. Upon reaching an agreement, the money is usually delivered via parachute drop-off onto the deck of the ship, and then split among the pirates. The amount that each of them would receive is a fixed fraction of the total ransom, and it would vary depending on the task [7]. About half of the pot would go to the actual men boarding the ship, one third to the investors financing the operation, and a sixth to everyone else assisting with logistics and enforcement.

We note that although 2017 saw a spike in pirate activities in the Gulf of Aden, this region seems to be no longer affected at same scale as it used to be during the 2000's [13]. According to the latest reports on encounters by the US government (Figure 1B) and the International Maritime Bureau of the International Chamber of Commerce (ICC-IMB), most encounters are now reported to take place in the Gulf of Guinea and Southeast Asia [25]. The business model of piracy in these regions, however, differs from the Somali pirates.

Pirates in the Gulf of Guinea follow a similar approach when it comes to intercepting a vessel. The difference comes after they have successfully hijacked the ship. Specifically, besides hijacking the vessel and its crew, these pirates appear to focus on kidnapping only a subset of crew members for ransom [25]. Another regular practice in this region is the robbery of cargo, especially liquid fuel [45].

Pirate encounters in Southeast Asia seem to follow a variation of the previous business model. According to recent reports, and in addition to the practices listed above, encounters include large-scale and sophisticated operations targeted at siphoning fuel from tanker vessels [46]. In this type of attack, vessels are also approached and hijacked, but then they are steered towards a siphoning facility on the shore that retrieves the entire cargo. Under this model, the crew and the ship are usually freed several days after a successful encounter [25].

Finally, pirate and armed-robbery encounters have increased along the Venezuelan and northern Colombian coasts, especially in areas such as the near-shore islands of Venezuela [29]. Economic distress in Venezuela (and parts of northern Colombia) is a key driver, where opportunistic offenders target private yachts and pleasure craft, frequently boarding to seize

cash, groceries, electronics and other easily carried valuables. To date these incidents appear generally sporadic and focused on smaller craft rather than large cargo vessels or full-scale hijackings. In the broader Caribbean there have been instances of commercial ship boarding, kidnapping of crewmembers, or ransom demands near Haiti [47].

B Supporting materials for regression analysis

In this section, we provide supporting material for the regression analyses referenced in the study. First, we provide the tables with the summary statistics for the data used in the grid and voyage regressions, respectively. Table B.1 shows that the average traffic per grid is highly variable across the globe, with the Gulf of Aden and Southeast Asia having much higher distance, occupancy time, voyages and unique vessels transiting in their respective areas than the rest of the world combined. For example, the average daily occupancy is about 43 and 204 hours in the Gulf of Aden and the Southeast Asia hotspots, respectively, while in the rest of the world the daily occupancy is 39.6 hours. This pattern persists for all the variables in the dataset, though there is considerable spread among all sub-samples and variables.

Table B.2 shows that when analyzed at the voyage level, the pattern is slightly modified. Here, in average, vessels crossing hotspots travel longer distances and for more time than vessels not crossing through hotspots, though there is also a relatively high degree of spread on the voyage features. Importantly, the hotspots with the highest mean observed piracy encounters in the preceding three months along routes take place in the Gulf of Guinea. The distribution of the remaining variables in the analysis (i.e., costs and emissions) follow directly from these observed features.

Second, we provide the regression tables not presented in the main text. The results for the linear average effect of piracy on fuel, labor, and total operational costs (in thousands of US dollars) are stacked in Table B.3. Across all samples, the results show that path adjustments increase fuel cost the most. One additional encounter relates to hundreds or thousands of dollars in additional fuel spent. These estimates are consistent with path adjustments. The results also suggest that vessels passing through the Gulf of Aden face the biggest burden with an additional US\$12 thousand per encounter, while those in the Gulf of Guinea face the least.

These adjustments are also meaningful in terms of labor cost. The effects of additional encounters are positive and significant, but at most half of the adjustment cost when compared to additional fuel consumption. We note that this result is consistent across samples.

We estimate the effect of piracy on total operational costs by aggregating both fuel and labor costs. These results are reported in Panel (C) of Table B.3, and suggest that the average increase in operational costs due to avoidance measures per additional pirate encounter ranges

from over US\$1,400 in the Gulf of Guinea to over US\$13,600 in the Gulf of Aden. Globally, this effect averages down to about US\$2,500 for each additional pirate encounter.

Finally, the linear average effects of piracy on emissions are stacked in Table B.4 for CO₂, NO_x, and SO_x, respectively. As expected from previous results, excessive fuel consumption leads to excessive emissions across the spectrum of relevant pollutants. In particular, increases in CO₂ range from 9 to 56 tons per voyage per past pirate encounter. NO_x and SO_x emissions due to piracy are relatively less voluminous, though this is a direct consequence of their significantly smaller concentrations in bunker fuel relative to carbon. Nonetheless, regression estimates point to dozens of kilograms, and hundreds in the case of the Gulf of Aden, of excess pollutants emitted due to the presence of pirates.

 ${\bf Table~B.1:~Summary~Statistics~for~Daily~Ship~Transit~by~Grid~Cell.}$

	Distance (km)	Occupancy (hr)	Voyages (#)	Unique vessels (#)			
Gulf of A	.den						
Mean	1,031.4	42.9	17.7	17.6			
SD	1,151.8	49.5	21.6	21.3			
Median	503.8	21.2	7.0	7.0			
Max	$4,\!436.4$	315.6	128.0	124.0			
Gulf of Guinea							
Mean	173.9	16.0	4.5	4.4			
SD	189.7	21.2	4.3	4.2			
Median	123.0	8.2	3.0	3.0			
Max	1,982.6	189.1	30.0	29.0			
Southeast Asia							
Mean	3,430.6	204.2	65.7	64.3			
SD	4,614.7	252.6	89.0	87.8			
Median	773.9	70.7	15.0	15.0			
Max	27,877.9	1,303.2	332.0	331.0			
Rest of the World							
Mean	483.9	39.6	11.6	11.2			
SD	913.5	68.6	19.8	19.5			
Median	239.2	19.7	7.0	6.0			
Max	12,766.6	882.7	195.0	190.0			

 ${\bf Table~B.2:~Summary~Statistics~for~Individual~Voyage~Features.}$

	Distance (km)	Time (hr)	Speed (km/hr)	Encounters (#/3 mo)
Gulf of A	den			
Mean	1,753.3	94.6	18.7	0.5
SD	3,060.6	217.5	7.4	1.2
Min	0.2	0.0	0.0	0.0
Max	421,538.8	37,861.1	115.5	25.0
Gulf of G	uinea			
Mean	3,014.9	149.6	20.1	4.6
SD	4,040.2	238.4	7.5	5.8
Min	0.1	0.0	0.0	0.0
Max	$468,\!276.4$	$33,\!372.3$	58.6	45.0
Southeast	Asia			
Mean	1,130.7	65.5	17.7	1.9
SD	2,768.4	266.8	6.6	5.0
Min	0.1	0.0	0.0	0.0
Max	813,656.8	$51,\!409.2$	130.2	44.0
Rest of th	ne World			
Mean	608.8	30.9	21.5	0.1
SD	1,506.3	102.0	8.3	0.6
Min	0.0	0.0	0.0	0.0
Max	464,388.8	53,031.0	1,060.9	27.0

Table B.3: Effect of Past Pirate Encounters on Shipping Cost.

	Global	G. of Aden	G. of Guinea	S.E. Asia
Panel (A): Fuel Cost ((TUSD)			
Encounters (7 day)	2.07*** (0.25)	12.08*** (1.14)	0.98*** (0.20)	1.64*** (0.29)
Panel (B): Labor Cost	(TUSD)			
Encounters (7 day)	0.41*** (0.04)	1.57*** (0.16)	0.49*** (0.03)	0.31*** (0.05)
Panel (C): Total Cost	(TUSD)			
Encounters (7 day)	2.48*** (0.28)	13.68*** (1.25)	1.46*** (0.21)	1.95*** (0.32)
Observations	26,304,136	984,899	341,556	6,254,926
Hotspot FE	X	•	•	•

^{*} p < 0.1, ** p < 0.05, *** p < 0.01 The unit of observation is a voyage. Each panel examines a calculated cost in terms of fuel cost, labor cost, and total cost as the sum of both. All coefficients are in thousands of US\$. The sample spans from 2013 to 2021. Every column is a different sample: Global is the analysis using the whole sample. G. of Aden, S.E. Asia, and G. of Guinea restrict the sample to vessels passing through one of the hotspots, respectively. Every panel-column combination is a different regression analysis. Encounters (7 day) is the count of pirate encounters recorded in the projected path of the vessel in the preceding 7 days from the departure date using a 5 degree spatial footprint. Controls include average wind speed along the voyage, the wind-resistance index, and wave height. Fixed effects include country-to-country combination, vessel type, vessel size, hotspot, and a battery of month by year and top port-to-port combination for country-to-country combination dummies.

Table B.4: Effect of Past Pirate Encounters on Shipping Emissions.

	Global	G. of Aden	G. of Guinea	S.E. Asia
Panel (A): CO2 (tons))			
Encounters (7 day)	9.66*** (1.08)	55.76*** (5.60)	8.92*** (0.75)	7.13*** (1.11)
Panel (B): NOx (kg)				
Encounters (7 day)	243.90*** (27.58)	1438.79*** (145.08)	222.30*** (19.63)	179.03*** (28.11)
Panel (C): SOx (kg)				
Encounters (7 day)	201.06*** (22.58)	1160.88*** (116.62)	185.67*** (15.69)	148.38*** (23.05)
Observations	26,777,022	1,003,520	346,715	6,377,789
Hotspot FE	X	•	•	•

^{*} p < 0.1, *** p < 0.05, **** p < 0.01 The unit of observation is a voyage. Each panel examines a calculated emission in terms of CO2 (tons), NOx (kg), and SOx (kg). The sample spans from 2013 to 2021. Every column is a different sample: Global is the analysis using the whole sample. G. of Aden, S.E. Asia, and G. of Guinea restrict the sample to vessels passing through one of the hotspots, respectively. Every panel-column combination is a different regression analysis. Encounters (7 day) is the count of pirate encounters recorded in the projected path of the vessel in the preceding 7 days from the departure date using a 5 degree spatial footprint. Controls include average wind speed along the voyage, the wind-resistance index, and wave height. Fixed effects include country-to-country combination, vessel type, vessel size, hotspot, and a battery of month by year and top port-to-port combination for country-to-country combination dummies.

C Counterfactual costs and emissions

We use the fully specified global model (5° grid, 7 day window) to predict voyage-level fuel and labor costs, as well as emissions of CO_2 , NO_x , and SO_x . We make predictions using the observed number of pirate encounters and a counterfactual of no pirate encounters at all. We then take the difference between these two predictions to obtain a voyage-level estimate of the additional fuel and labor costs, and emissions of each pollutant. We then calculate the total annual costs and emissions across all voyages. These results are shown in Table C.5 and Table C.6, where we also provide information disaggregated by hotspot.

Having matched each voyage to its additional costs and emissions, we then divide a voyage's cost (or emissions) across all $0.5^{\circ} \times 0.5^{\circ}$ grid cells along which the vessel transited. For each grid cell, we calculate the total excesscosts (fuel + labor) or emissions of each pollutant. We then take the average across all years (2012-2023) and use these data to produce maps shown in Figure 4A.

We monetize the environmental impacts caused by additional emission of local and global air pollutants using their social cost. Specifically, we use estimates provided by the Interagency Working Group on Social Cost of Greenhouse Gases [26], which suggest that an additional ton of CO_2 or NO_x induce damages valued at US\$51 and US\$18,000 (in 2020 US\$ assuming a 3% discount rate). For SO_x we use estimates from Mier, Adelowo, and Weissbart [34], which indicates an additional ton of SO_2 induces damages of US\$14,694 (in 2020 US\$). We then aggregate all information by ASAM region, and produce the bar chart shown in Figure 4B.

Table C.5: Total Costs of Piracy to the Shipping Industry.

	2012	2013	2014	2015	2016	2017	2018	2019	2020	2021	2022	2023
Fuel (Million US	SD)											
Global	774	1,265	1,496	1,794	851	930	577	424	1,358	1,143	1,241	1,504
G. of Aden	105	74	40	11	30	87	27	20	36	40	30	25
G. of Guinea	83	111	65	49	88	90	103	47	124	84	39	34
Southeast Asia	550	1,007	1,366	1,695	597	671	367	313	1,089	957	1,113	1,404
Labor (Million V	USD)											
Global	154	251	297	356	169	184	114	84	269	227	246	324
G. of Aden	21	15	8	2	6	17	5	4	7	8	6	6
G. of Guinea	16	22	13	10	17	18	20	9	25	17	8	7
Southeast Asia	109	200	271	336	118	133	73	62	216	190	221	302
Total (Million U	$^{\mathrm{ISD}}$											
Global	929	1,518	1,796	2,153	1,022	1,117	692	509	1,630	1,372	1,490	1,805
G. of Aden	126	89	48	13	37	105	32	24	44	48	36	30
G. of Guinea	100	133	78	59	105	107	124	56	149	101	47	41
Southeast Asia	660	1,208	1,639	2,034	716	805	440	376	1,307	1,149	1,336	1,685

Table C.6: Total Emission of Air Pollutants due to Piracy

	2012	2013	2014	2015	2016	2017	2018	2019	2020	2021	2022	2023
CO ₂ (Thousand	metric	tons)										
Global	3,528	5,763	6,818	8,176	3,880	4,240	2,628	1,932	6,188	5,209	5,656	7,456
G. of Aden	478	339	180	51	139	399	123	91	166	184	136	149
G. of Guinea	379	505	295	224	399	408	471	214	565	382	177	166
Southeast Asia	2,505	4,588	6,224	7,722	2,719	3,057	1,672	1,428	4,963	4,361	5,073	6,942
NOx (Metric to	ns)											
Global	88,892	145,220	171,819	206,034	97,772	106,839	66,233	48,696	155,932	131,270	142,535	187,884
G. of Aden	12,040	8,548	4,545	1,277	3,495	10,044	3,109	2,291	4,182	4,637	3,421	3,748
G. of Guinea	9,548	12,729	7,438	5,632	10,066	10,283	11,870	5,400	14,250	9,618	4,468	4,172
Southeast Asia	63,122	115,622	156,843	$194,\!592$	68,506	77,047	42,121	35,982	125,063	109,903	127,832	174,932
SOx (Metric to	ns)											
Global	73,444	119,983	141,960	170,229	80,781	88,272	54,723	40,233	128,834	108,458	117,765	155,233
G. of Aden	9,948	7,063	3,755	1,055	2,888	8,299	2,569	1,893	3,455	3,831	2,827	3,097
G. of Guinea	7,889	10,517	6,145	4,654	8,317	8,496	9,807	4,461	11,774	7,946	3,692	3,447
Southeast Asia	$52,\!153$	95,529	$129,\!587$	160,775	56,600	63,657	$34,\!801$	29,729	103,329	90,804	$105,\!617$	$144,\!532$

D Robustness tests

This section shows robustness checks for all of the empirical results: how pirate encounters affect total shipping traffic within spatial grids, and how pirate encounters affect the features of individual voyages. The two sets of robustness checks largely follow the same pattern. Pirate encounters reduce traffic within grid cells. These adjustments result in adjustments at the individual voyage level, which is then demonstrated by increase in the average total distance time traveled for the same port-to-port combination.

D.1 Grid-level analysis

First, we show that our results are driven by shippers avoiding an area with known presence of pirates rather than by other behavioral adaptations. For example, a shipping captain may decide to disable the AIS transponder onboard their vessel as a way to conceal their presence. To test for this, we use a publicly available dataset of known AIS disabling events. For details on the data, see [52]. Essentially, we match known positions where a vessel "went dark" to all grid cells with at least one reported pirate encounter. As with our main-text specifications, we regress the number of AIS disabling events on a dummy variable indicating whether the day was before or after a reported pirate encounter. Our results are shown in Table D.7. At a global level, we do not find enough evidence suggesting that the number of AIS-disabling events increases within the 7 days following a pirate encounter. In the Gulf of Aden we retrieve a non-significant coefficient of -0.001. In the Gulf of Guinea we see a moderate increase, with a coefficient of 0.002 indicating that, on average, there is a 2% increase in the number of disabling events following an encounter. We do not estimate the effect for the Southeast Asia hotspot because the outcome variable was always 0 (i.e., there were no disabling events within attacked hotspots).

Second, we show that our grid-level results are not driven by choices of the spatial resolution for our analysis. To test for this, we repeat our analysis but this time using two other resolutions. Our main-text results use a 0.5°-by-0.5° grid. Figure D.1 shows results for two other resolutions. Namely, we increase the spatial resolution to 0.1°-by-0.1° or decrease it to 1°-by-1°. Both resolutions show similar patterns, with the finer grid showing longer lasting and sharper effects than those associated with the coarser grid.

Table D.7: Effect of Pirate Attacks on Grid Cell Shipping Activity.

	Global	G. of Aden	G. of Guinea
Post-Attack	0.000 (0.000)	-0.001 (0.001)	0.002** (0.001)

^{*} p < 0.1, ** p < 0.05, *** p < 0.01 The unit of observation is a grid cell-day. Each each column represents a different geographic region. The Southeast Asia hotspot is excluded because there were no disabling events detected within attacked pixels. Post-Attack is a binary indicator equal to 1 for days on or after a pirate attack in the grid cell. The analysis uses a 7-day window around attacks to identify pre- and post-attack periods. All regressions include grid cell, year-month, and day of week fixed effects. Standard errors are Conley standard errors (50km cutoff) and reported in parentheses.

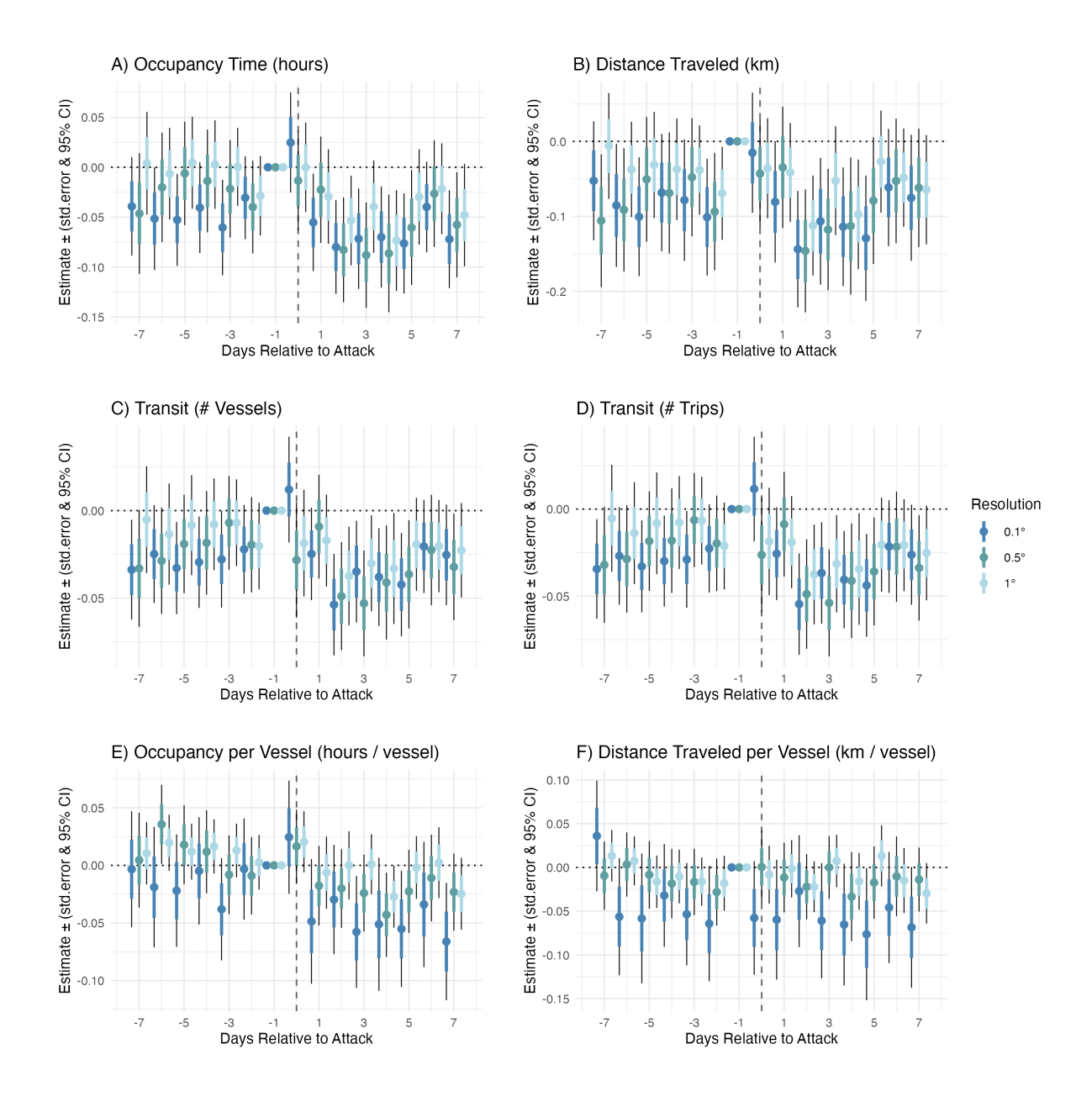


Figure D.1: Dynamic effects of piracy on ship transit for three different grid resolutions. The unit of observation is a grid cell-day. Each inset examines a different shipping activity measure. The horizontal axis shows time relative to the day of the attack. The vertical axis shows the magnitude of the effect. Points are coefficient estimates showing change in shipping activity. Different colors indicate different resolutions. The thick colored portion of the error bars show Conley standard errors (50km cutoff), and the thin black portion shows 95% Confidence Intervals.

D.2 Voyage-level analysis

Here we present evidence of the robustness of the voyage analysis to several modeling and identification assumptions. First, we show robustness to different sets of fixed effects in tabular form. The estimates are sensitive to the inclusion of country-to-country fixed effects, but this is expected as the length and specific paths of each route are bound to vary widely across combinations. The suite of results are included in Tables D.8 to D.16. Overall, the results are highly robust to the addition of vessel, hotspot and top route fixed effects. The results are also robust to the inclusion of weather controls in the form of wind speed, wind-resistance index, and wave height.

We note that over 6 million voyages are dropped when adding weather controls. This is because spatiotemporal wind speed data is available globally from ERA5. Wind vector data meanwhile, is a composite of both wind speed and vessel heading. Heading is usually, but not always, broadcast during the transmission of AIS messages, meaning that a value for the wind vector cannot be calculated for some voyages where the vessel does not broadcast its heading. Wave height data from ERA5 is restricted to the ocean, meaning that its value may be missing for trips that occurred exclusively within some inland areas such as some rivers and lakes. Wave height data are also limited in areas that are predominantly covered by sea ice, and thus may be missing for trips that occur exclusively in these areas.

We also note that about 600,000 observations are missing from the cost regressions, when compared to the voyage feature regressions. This is because 2,816 vessels are missing engine information, and we are only able to acquire fuel prices up to October 19, 2023. Some of these missing observations overlap with the ones missing weather information, so the difference between the fully specified models is about 500,000.

Second, we show robustness to i) using a rolling window of 7, 15, and 30 days, as well as the use of a global 3°x3°, 5°x5°, and 7°x7° grid to construct the past encounters variable. This approach allows us to test the temporal and spatial sensitivity of our analysis and the results are shown in Figure D.2. The results show that the effect of recent encounters diminishes when longer time windows are considered and that working with larger spatial footprints (i.e., 7°x7°) tends to attenuate results toward zero. For completeness, we will maintain these variations in temporal and spatial scale in all of the analyses below.

Third, we show robustness of the results to the categorization of cargo vessels. In the main analysis, we use the best available vessel class for each individual vessel as categorized by Global Fishing Watch. This "best available" approach uses the vessel class provided by official registries where available, and infers vessel class using a neural network when registries are not available [30]. As a robustness check, we restrict the analysis to work with: 1) vessels that are always categorized as cargo vessels according to official registries; as well as 2) expand it as those who are categorized in official registries as being cargo vessels at least once. These results are shown in Figure D.3 and Figure D.4 and are virtually unchanged with respect to the results in the main analysis, though minimal changes around zero are detected for the speed analysis. We reiterate that the magnitudes detected for speed are practically meaningless.

Fourth, we show robustness to the definition of our explanatory variable. For each voyage, we calculate the total number of unique encounters that occurred along all previously traveled paths (i.e., surrogate trips), as well as the chosen path, for each port-to-port route within the preceding months of a voyage's departure. This represents, for any given voyage departure date for any given port-to-port route, the captain's assessment of the prevalence of piracy along the universe of potential paths that have been recently traveled along the route. We call this variable "Total Number of Encounters." The results from this test are shown in Figure D.5 and are consistent with the main analysis, though there is considerable attenuation. This is expected, as the marginal impact of an additional pirate encounter diminishes as the potential area of paths along a route increases.

In addition, for each voyage we calculate the average number of unique pirate encounters that occurred along all previously traveled paths (i.e., surrogate trips) for that port-to-port route within a time window. This represents, for any given voyage departure date for any given port-to-port route, the captain's expectation of how many encounters they might expect could occur along the path. We call this variable "Average Number of Encounters." This analysis is presented in Figure D.6, and shows considerable attenuation. Positive effects in terms of distance are detected, except in Southeast Asia. Effects in terms of time are mostly dissipated. This result is expected, as it is again easy to see the marginal impact of an additional pirate encounter diminishes further as its effect is now diluted by a considerably increase in the spatial footprint considered, over the number of voyages that took place before.

We also show robustness of the results to the addition of speed and days since the last encounter along a route as *covariates*. The results are shown in Figure D.7, and are practically unchanged. These results provide support that the omission of voyage speed or other short-term risk features does not bias the main adjustment estimates.

Table D.8: Effect of Past Pirate Encounters on Voyage Distance.

	(1)	(2)	(3)	(4)	(5)	(6)
Encounters (3 day)	734.51***	808.51***	67.11***	65.30***	64.36***	64.91***
	(58.08)	(51.18)	(6.76)	(6.69)	(6.67)	(6.64)
Wind Speed (m/s)		138.77***	2.53	3.92	0.37	1.28
		(24.68)	(3.15)	(2.83)	(2.87)	(2.82)
Wind Resistance Index (m/s)		-14.25***	-8.04***	-7.81***	-7.98***	-8.11***
		(3.03)	(0.99)	(0.94)	(0.95)	(0.93)
Wave Height (m)		1,131.33***	273.23***	272.76***	255.70***	251.69***
		(97.14)	(17.01)	(14.59)	(16.36)	(15.95)
Observations	33,015,555	26,777,022	26,777,022	26,777,022	26,777,022	26,777,022
Country Combo. FE			X	X	X	X
Vessel Type FE				X	X	X
Vessel Size FE				X	X	X
Hotspot FE					X	X
Top Route FE						X
Month-by-Year FE	X	X	X	X	X	X

^{*} p < 0.1, ** p < 0.05, *** p < 0.01 The unit of observation is a voyage. The sample spans from 2013 to 2021. Every column is a different specification. Encounters (7 day) is the count of pirate encounters recorded in the projected path of the vessel in the preceding 7 days from the departure date using a 5 degree spatial footprint. Controls include average wind speed along the voyage, the wind-resistance index, and wave height. Fixed effects include country-to-country combination, vessel type, vessel size, hotspot, and a battery of month by year and top port-to-port combination for country-to-country combination dummies.

Table D.9: Effect of Past Pirate Encounters on Voyage Time.

	(1)	(2)	(3)	(4)	(5)	(6)
Encounters (3 day)	34.45***	37.21***	3.25***	3.18***	3.14***	3.18***
	(2.67)	(2.40)	(0.34)	(0.33)	(0.33)	(0.33)
Wind Speed (m/s)		6.50***	-0.23	-0.21	-0.37***	-0.30**
		(1.11)	(0.16)	(0.14)	(0.14)	(0.14)
Wind Resistance Index (m/s)		-0.37***	-0.15***	-0.15***	-0.16***	-0.17***
		(0.14)	(0.05)	(0.05)	(0.05)	(0.05)
Wave Height (m)		47.27***	15.06***	15.09***	14.25***	13.92***
		(4.46)	(0.90)	(0.80)	(0.90)	(0.87)
Observations	33,015,555	26,777,022	26,777,022	26,777,022	26,777,022	26,777,022
Country Combo. FE			X	X	X	X
Vessel Type FE				X	X	X
Vessel Size FE				X	X	X
Hotspot FE					X	X
Top Route FE						X
Month-by-Year FE	X	X	X	X	X	X

^{*} p < 0.1, ** p < 0.05, *** p < 0.01 The unit of observation is a voyage. The sample spans from 2013 to 2021. Every column is a different specification. Encounters (7 day) is the count of pirate encounters recorded in the projected path of the vessel in the preceding 90 days from the departure date using a 5 degree spatial footprint. Controls include average wind speed along the voyage, the wind-resistance index, and wave height. Fixed effects include country-to-country combination, vessel type, vessel size, hotspot, and a battery of month by year and top port-to-port combination for country-to-country combination dummies.

Table D.10: Effect of Past Pirate Encounters on Voyage Speed.

	(1)	(2)	(3)	(4)	(5)	(6)
Encounters (7 day)	0.85***	0.75***	0.09***	0.06***	0.06***	0.05***
	(0.11)	(0.08)	(0.01)	(0.01)	(0.01)	(0.01)
Wind Speed (m/s)		-0.03	0.00	0.04***	0.03**	0.02*
		(0.06)	(0.02)	(0.01)	(0.01)	(0.01)
Wind Resistance Index (m/s)		-0.11***	-0.08***	-0.07***	-0.07***	-0.07***
		(0.02)	(0.01)	(0.01)	(0.01)	(0.01)
Wave Height (m)		1.79***	-0.01	0.02	-0.03	0.00
		(0.19)	(0.11)	(0.07)	(0.07)	(0.07)
Observations	33,015,555	26,777,022	26,777,022	26,777,022	26,777,022	26,777,022
Country Combo. FE			X	X	X	X
Vessel Type FE				X	X	X
Vessel Size FE				X	X	X
Hotspot FE					X	X
Top Route FE						X
Month-by-Year FE	X	X	X	X	X	X

^{*} p < 0.1, ** p < 0.05, *** p < 0.01 The unit of observation is a voyage. The sample spans from 2013 to 2021. Every column is a different specification. Encounters (7 day) is the count of pirate encounters recorded in the projected path of the vessel in the preceding 7 days from the departure date using a 5 degree spatial footprint. Controls include average wind speed along the voyage, the wind-resistance index, and wave height. Fixed effects include country-to-country combination, vessel type, vessel size, hotspot, and a battery of month by year and top port-to-port combination for country-to-country combination dummies.

Table D.11: Effect of Past Pirate Encounters on Fuel Cost.

	(1)	(2)	(3)	(4)	(5)	(6)
Encounters (7 day)	16.60***	18.40***	2.23***	2.10***	2.07***	2.07***
	(1.35)	(1.19)	(0.24)	(0.25)	(0.25)	(0.25)
Wind Speed (m/s)		3.18***	0.15*	0.24***	0.16*	0.16*
		(0.55)	(0.09)	(0.09)	(0.09)	(0.09)
Wind Resistance Index (m/s)		-0.40***	-0.19***	-0.17***	-0.17***	-0.17***
		(0.07)	(0.03)	(0.02)	(0.02)	(0.02)
Wave Height (m)		25.19***	5.53***	4.73***	4.35***	4.37***
		(2.26)	(0.43)	(0.35)	(0.37)	(0.37)
Observations	32,440,604	26,304,136	26,304,136	26,304,136	26,304,136	26,304,136
Country Combo. FE			X	X	X	X
Vessel Type FE				X	X	X
Vessel Size FE				X	X	X
Hotspot FE					X	X
Top Route FE						X
Month-by-Year FE	X	X	X	X	X	X

^{*} p < 0.1, ** p < 0.05, *** p < 0.01 The unit of observation is a voyage. The sample spans from 2013 to 2021. Every column is a different specification. Encounters (7 day) is the count of pirate encounters recorded in the projected path of the vessel in the preceding 7 days from the departure date using a 5 degree spatial footprint. Controls include average wind speed along the voyage, the wind-resistance index, and wave height. Fixed effects include country-to-country combination, vessel type, vessel size, hotspot, and a battery of month by year and top port-to-port combination for country-to-country combination dummies.

Table D.12: Effect of Past Pirate Encounters on Labor Cost.

	(1)	(2)	(3)	(4)	(5)	(6)
Encounters (7 day)	4.51***	4.93***	0.42***	0.41***	0.40***	0.41***
	(0.36)	(0.32)	(0.04)	(0.04)	(0.04)	(0.04)
Wind Speed (m/s)		0.75***	-0.04*	-0.03*	-0.05***	-0.04**
		(0.14)	(0.02)	(0.02)	(0.02)	(0.02)
Wind Resistance Index (m/s)		-0.05***	-0.02***	-0.02***	-0.02***	-0.02***
		(0.02)	(0.01)	(0.01)	(0.01)	(0.01)
Wave Height (m)		6.90***	2.05***	2.04***	1.95***	1.91***
		(0.51)	(0.13)	(0.10)	(0.11)	(0.11)
Observations	32,440,604	26,304,136	26,304,136	26,304,136	26,304,136	26,304,136
Country Combo. FE			X	X	X	X
Vessel Type FE				X	X	X
Vessel Size FE				X	X	X
Hotspot FE					X	X
Top Route FE						X
Month-by-Year FE	X	X	X	X	X	X

^{*} p < 0.1, ** p < 0.05, *** p < 0.01 The unit of observation is a voyage. The sample spans from 2013 to 2021. Every column is a different specification. Encounters (7 day) is the count of pirate encounters recorded in the projected path of the vessel in the preceding 7 days from the departure date using a 5 degree spatial footprint. Controls include average wind speed along the voyage, the wind-resistance index, and wave height. Fixed effects include country-to-country combination, vessel type, vessel size, hotspot, and a battery of month by year and top port-to-port combination for country-to-country combination dummies.

Table D.13: Effect of Past Pirate Encounters on Total Cost.

	(1)	(2)	(3)	(4)	(5)	(6)
Encounters (7 day)	21.07***	23.29***	2.66***	2.50***	2.48***	2.48***
, , , ,	(1.70)	(1.49)	(0.28)	(0.28)	(0.28)	(0.28)
Wind Speed (m/s)	, ,	3.94***	0.11	0.21**	0.11	0.11
		(0.69)	(0.10)	(0.10)	(0.10)	(0.10)
Wind Resistance Index (m/s)		-0.45***	-0.21***	-0.18***	-0.19***	-0.19***
		(0.08)	(0.03)	(0.03)	(0.03)	(0.03)
Wave Height (m)		32.13***	7.58***	6.78***	6.29***	6.28***
		(2.76)	(0.52)	(0.42)	(0.45)	(0.44)
Observations	32,440,604	26,304,136	26,304,136	26,304,136	26,304,136	26,304,136
Country Combo. FE			X	X	X	X
Vessel Type FE				X	X	X
Vessel Size FE				X	X	X
Hotspot FE					X	X
Top Route FE						X
Month-by-Year FE	X	X	X	X	X	X

^{*} p < 0.1, ** p < 0.05, *** p < 0.01 The unit of observation is a voyage. The sample spans from 2013 to 2021. Every column is a different specification. Encounters (7 day) is the count of pirate encounters recorded in the projected path of the vessel in the preceding 7 days from the departure date using a 5 degree spatial footprint. Controls include average wind speed along the voyage, the wind-resistance index, and wave height. Fixed effects include country-to-country combination, vessel type, vessel size, hotspot, and a battery of month by year and top port-to-port combination for country-to-country combination dummies.

Table D.14: Effect of Past Pirate Encounters on CO2 Emissions.

	(1)	(2)	(3)	(4)	(5)	(6)
Encounters (7 day)	107.88***	120.08***	10.73***	9.82***	9.68***	9.66***
	(8.57)	(7.46)	(1.07)	(1.08)	(1.08)	(1.08)
Wind Speed (m/s)		20.78***	0.70	1.35***	0.81*	0.77*
		(3.69)	(0.47)	(0.45)	(0.44)	(0.44)
Wind Resistance Index (m/s)		-2.65***	-1.17***	-1.00***	-1.02***	-1.02***
		(0.42)	(0.15)	(0.14)	(0.14)	(0.14)
Wave Height (m)		167.67***	37.13***	31.77***	29.35***	29.53***
		(14.89)	(2.59)	(2.01)	(2.13)	(2.14)
Observations	33,015,555	26,777,022	26,777,022	26,777,022	26,777,022	26,777,022
Country Combo. FE			X	X	X	X
Vessel Type FE				X	X	X
Vessel Size FE				X	X	X
Hotspot FE					X	X
Top Route FE						X
Month-by-Year FE	X	X	X	X	X	X

^{*} p < 0.1, ** p < 0.05, *** p < 0.01 The unit of observation is a voyage. The sample spans from 2013 to 2021. Every column is a different specification. Encounters (7 day) is the count of pirate encounters recorded in the projected path of the vessel in the preceding 7 days from the departure date using a 5 degree spatial footprint. Controls include average wind speed along the voyage, the wind-resistance index, and wave height. Fixed effects include country-to-country combination, vessel type, vessel size, hotspot, and a battery of month by year and top port-to-port combination for country-to-country combination dummies.

Table D.15: Effect of Past Pirate Encounters on NOx Emissions.

	(1)	(2)	(3)	(4)	(5)	(6)
Encounters (7 day)	2,727.15***	3,040.51***	271.30***	248.32***	244.70***	243.90***
	(217.27)	(188.96)	(27.32)	(27.59)	(27.55)	(27.58)
Wind Speed (m/s)		525.30***	19.56	36.49***	22.67**	21.35*
		(93.97)	(12.10)	(11.63)	(11.32)	(11.40)
Wind Resistance Index (m/s)		-70.13***	-31.80***	-27.36***	-27.96***	-27.77***
		(10.58)	(4.05)	(3.68)	(3.67)	(3.68)
Wave Height (m)		4,290.47***	930.10***	791.55***	729.97***	735.81***
		(379.09)	(65.77)	(51.23)	(54.19)	(54.55)
Observations	33,015,555	26,777,022	26,777,022	26,777,022	26,777,022	26,777,022
Country Combo. FE			X	X	X	X
Vessel Type FE				X	X	X
Vessel Size FE				X	X	X
Hotspot FE					X	X
Top Route FE						X
Month-by-Year FE	X	X	X	X	X	X

^{*} p < 0.1, ** p < 0.05, *** p < 0.01 The unit of observation is a voyage. The sample spans from 2013 to 2021. Every column is a different specification. Encounters (7 day) is the count of pirate encounters recorded in the projected path of the vessel in the preceding 7 days from the departure date using a 5 degree spatial footprint. Controls include average wind speed along the voyage, the wind-resistance index, and wave height. Fixed effects include country-to-country combination, vessel type, vessel size, hotspot, and a battery of month by year and top port-to-port combination for country-to-country combination dummies.

Table D.16: Effect of Past Pirate Encounters on SOx Emissions.

	(1)	(2)	(3)	(4)	(5)	(6)
Encounters (7 day)	2,245.99***	2,500.02***	223.45***	204.53***	201.57***	201.06***
, , , , , , , , , , , , , , , , , , ,	(178.36)	(155.30)	(22.38)	(22.59)	(22.55)	(22.58)
Wind Speed (m/s)		432.61***	14.58	28.13***	16.86*	16.02*
		(76.88)	(9.85)	(9.42)	(9.18)	(9.23)
Wind Resistance Index (m/s)		-55.16***	-24.37***	-20.79***	-21.28***	-21.16***
		(8.65)	(3.21)	(2.88)	(2.87)	(2.88)
Wave Height (m)		3,490.85***	773.15***	661.46***	611.03***	614.75***
		(310.11)	(53.83)	(41.80)	(44.29)	(44.48)
Observations	33,015,555	26,777,022	26,777,022	26,777,022	26,777,022	26,777,022
Country Combo. FE			X	X	X	X
Vessel Type FE				X	X	X
Vessel Size FE				X	X	X
Hotspot FE					X	X
Top Route FE						X
Month-by-Year FE	X	X	X	X	X	X

^{*} p < 0.1, ** p < 0.05, *** p < 0.01 The unit of observation is a voyage. The sample spans from 2013 to 2021. Every column is a different specification. Encounters (7 day) is the count of pirate encounters recorded in the projected path of the vessel in the preceding 7 days from the departure date using a 5 degree spatial footprint. Controls include average wind speed along the voyage, the wind-resistance index, and wave height. Fixed effects include country-to-country combination, vessel type, vessel size, hotspot, and a battery of month by year and top port-to-port combination for country-to-country combination dummies.

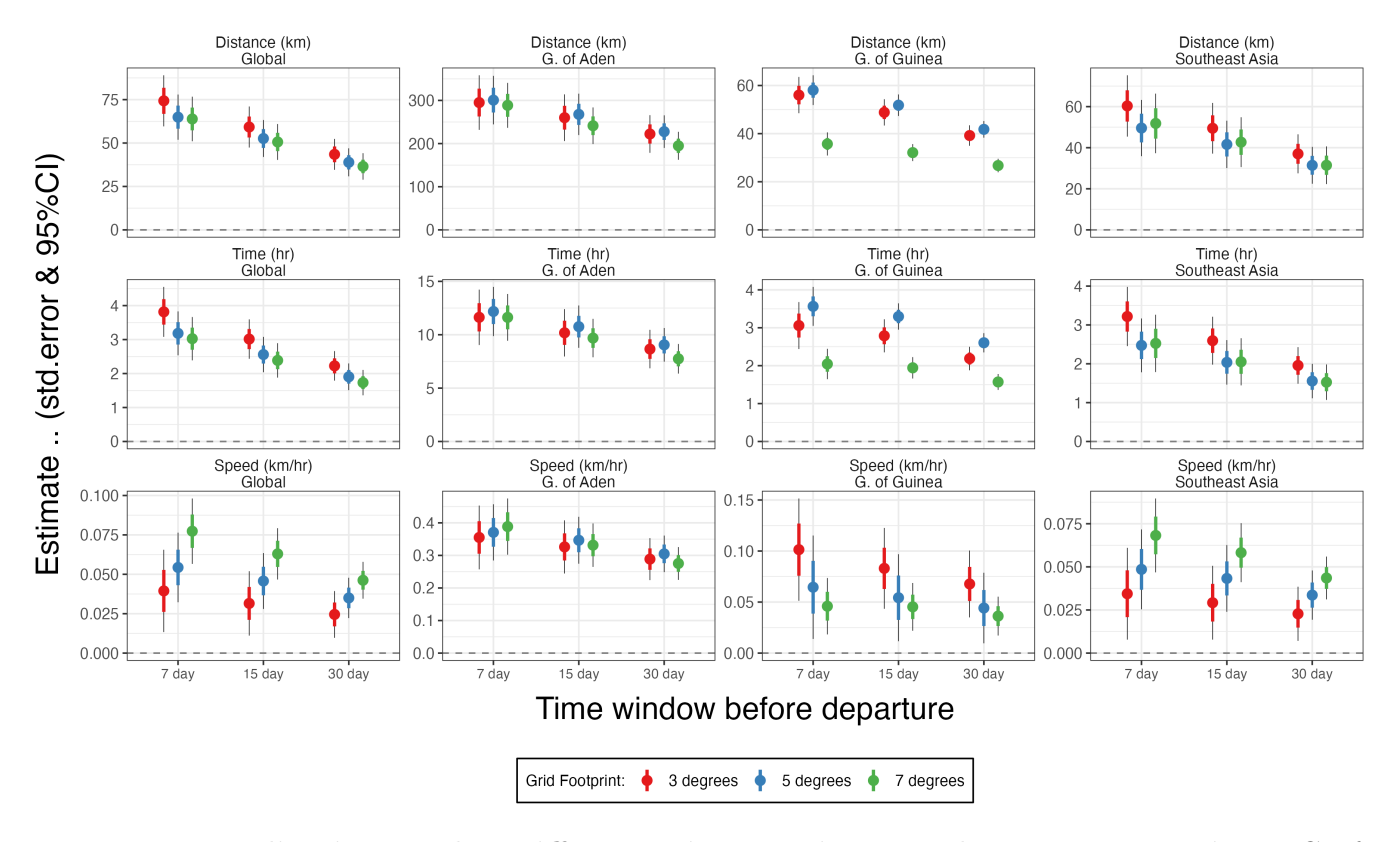


Figure D.2: Replication Under Different Time Horizons and Degree Footprints. Coefficients show the change in voyage features as a function of the number of pirate encounters in the preceding months. The analysis is conducted for all the variables and subsamples reported in the main text. Each plot shows the results for models using time windows of 7, 15, and 30 days, respectively. Each color shows results for models using a 3, 5, and 7° spatial footprint, respectively. The thick portion of error bars are the clustered standard errors, and the thin portion of error bars shows 95%CIs. Estimation, subsampling, specification, and clustering approach remain identical to those in Table 1.

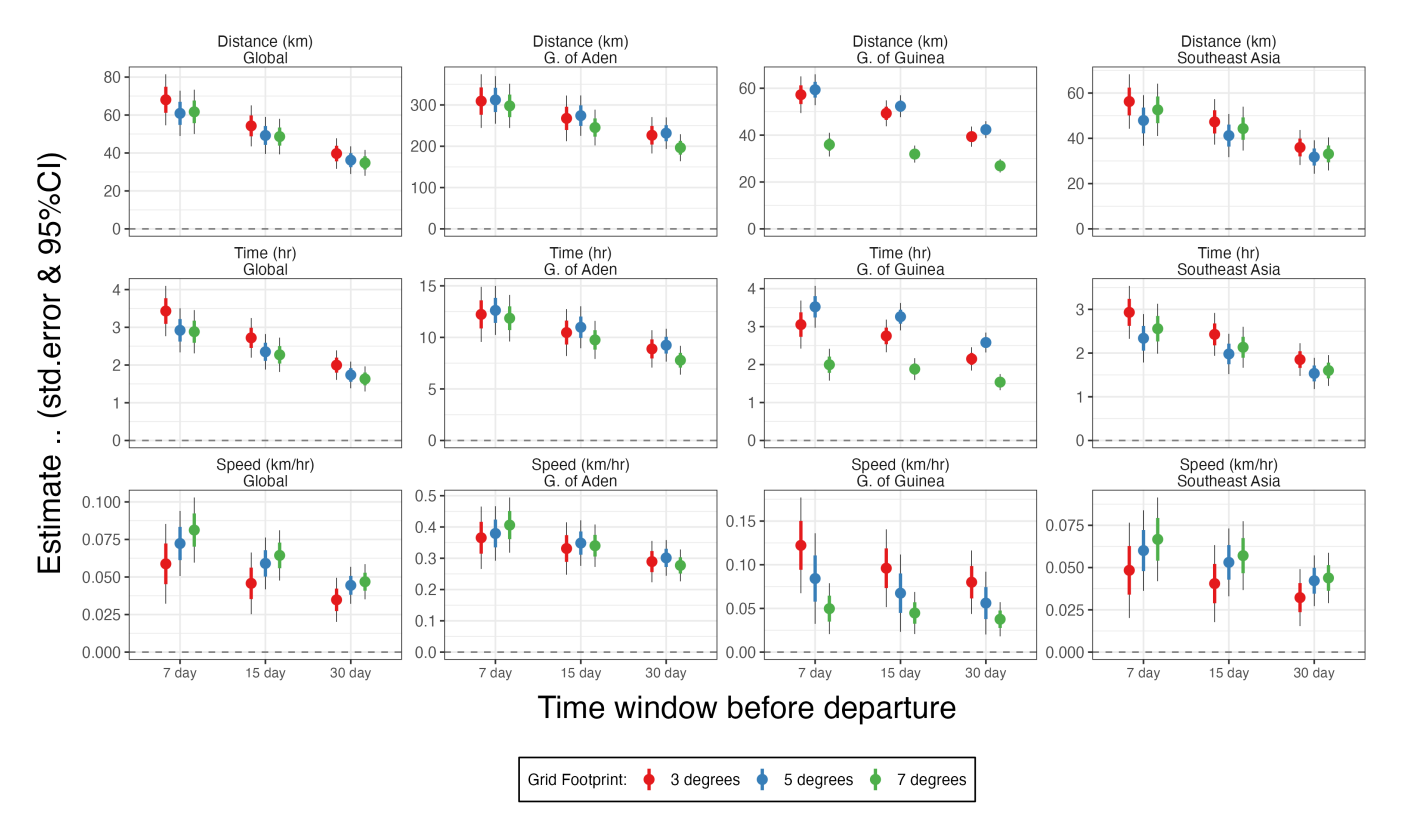


Figure D.3: Replication Under Different Time Horizons and Degree Footprints of Vessels Always Classified as Cargo. Coefficients show the change in voyage features as a function of the number of pirate encounters in the preceding months. The analysis is conducted for all the variables and subsamples reported in the main text. Each plot shows the results for models using time windows of 7, 15, and 30 days, respectively. Each color shows results for models using a 3, 5, and 7° spatial footprint, respectively. The thick portion of error bars are the clustered standard errors, and the thin portion of error bars shows 95%CIs. Estimation, subsampling, specification, and clustering approach remain identical to those in Table 1.

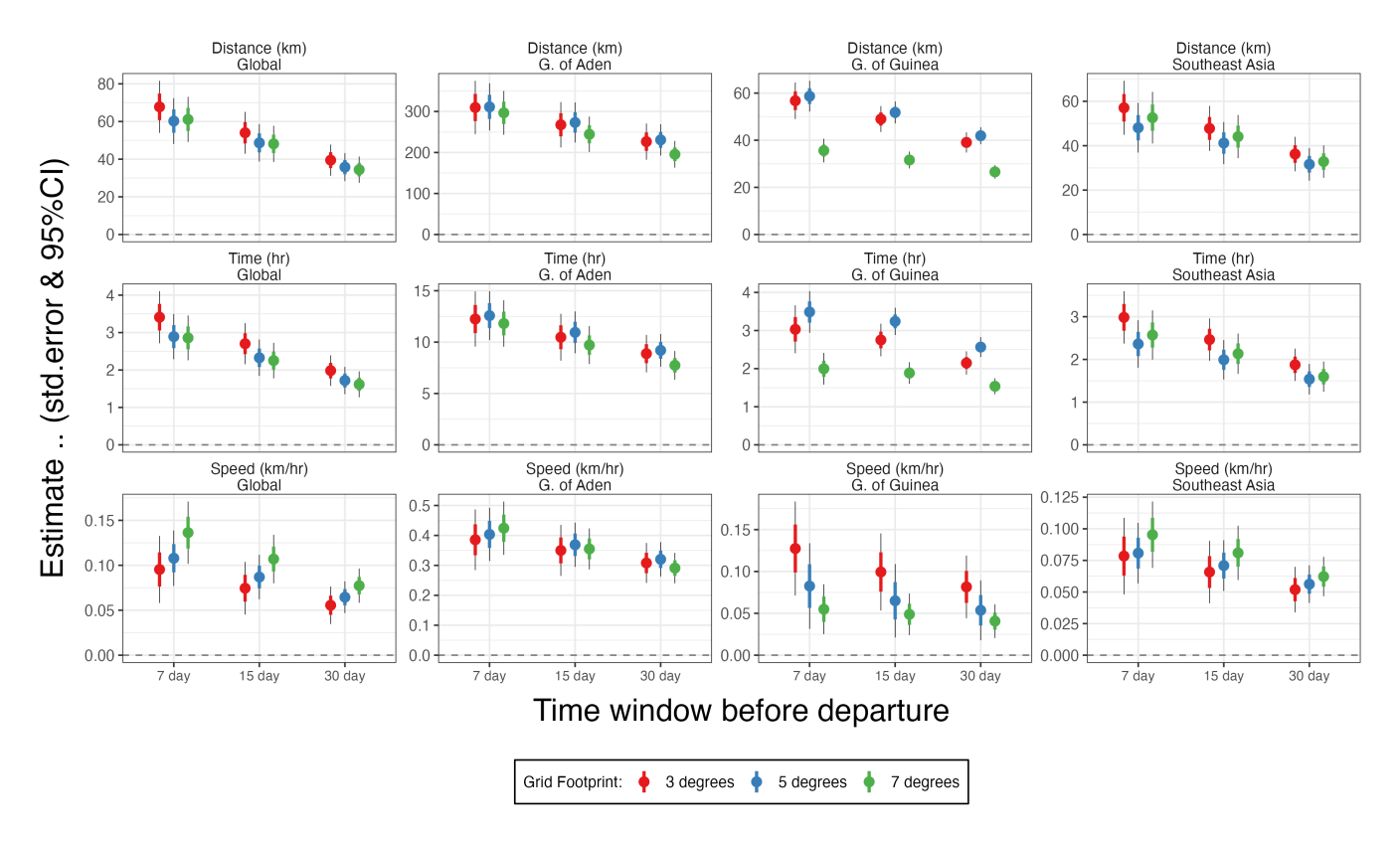


Figure D.4: Replication Under Different Time Horizons and Degree Footprints of Vessels at Least Once Classified as Cargo. Coefficients show the change in voyage features as a function of the number of pirate encounters in the preceding months. The analysis is conducted for all the variables and subsamples reported in the main text. Each plot shows the results for models using time windows of 7, 15, and 30 days, respectively. Each color shows results for models using a 3, 5, and 7° spatial footprint, respectively. The thick portion of error bars are the clustered standard errors, and the thin portion of error bars shows 95%CIs. Estimation, subsampling, specification, and clustering approach remain identical to those in Table 1.

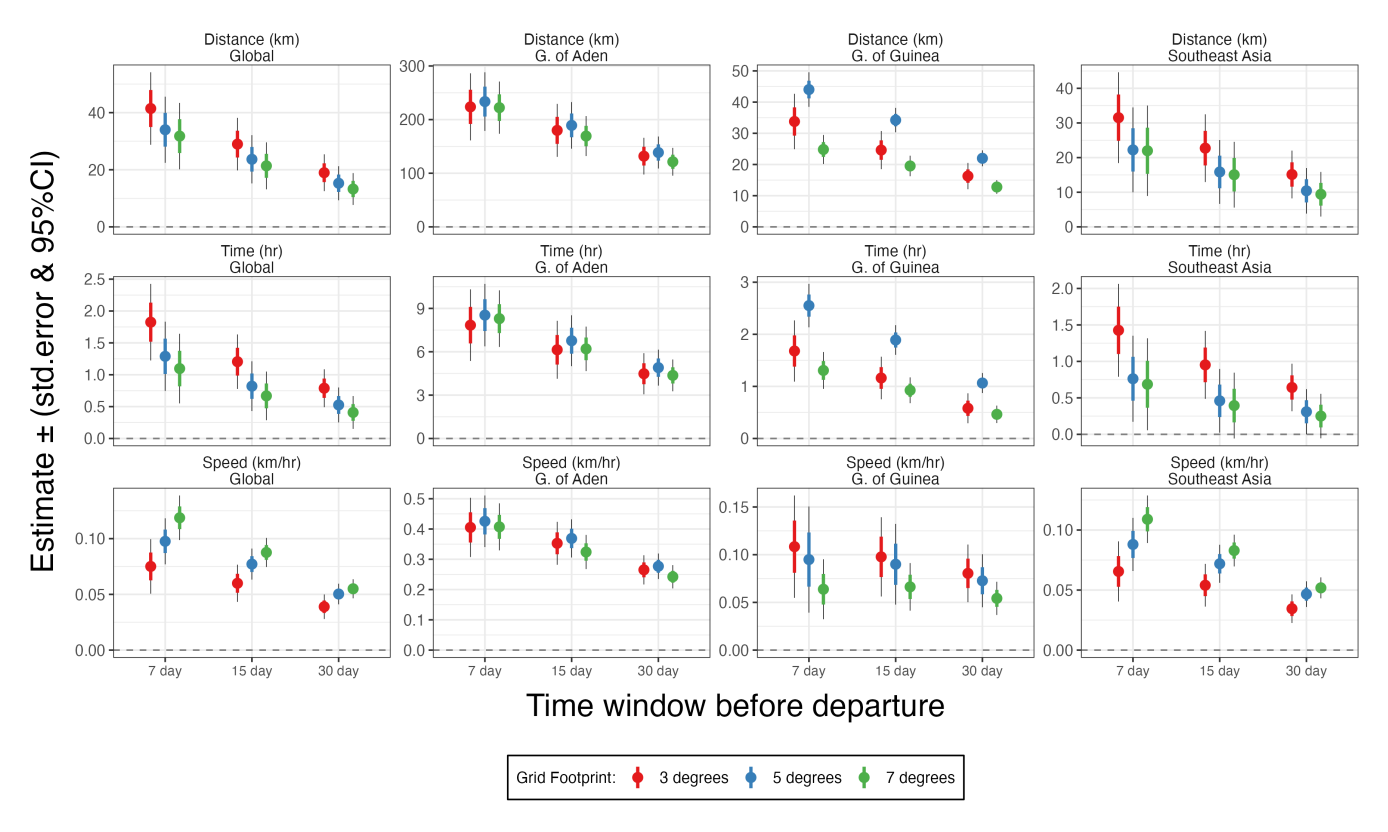


Figure D.5: Replication Using Total Number of Encounters Under Different Time Horizons and Degree Footprints. Coefficients show the change in voyage features as a function of the average number of pirate encounters experienced by other vessels in the preceding months. The analysis is conducted for all the variables and subsamples reported in the main text. Each plot shows the results for models using time windows of 7, 15, and 30 days, respectively. Each color shows results for models using a 3, 5, and 7° spatial footprint, respectively. The thick portion of error bars are the clustered standard errors, and the thin portion of error bars shows 95%CIs. Other than the explanatory variable, estimation, subsampling, specification, and clustering approach remain identical to those in Table 1.

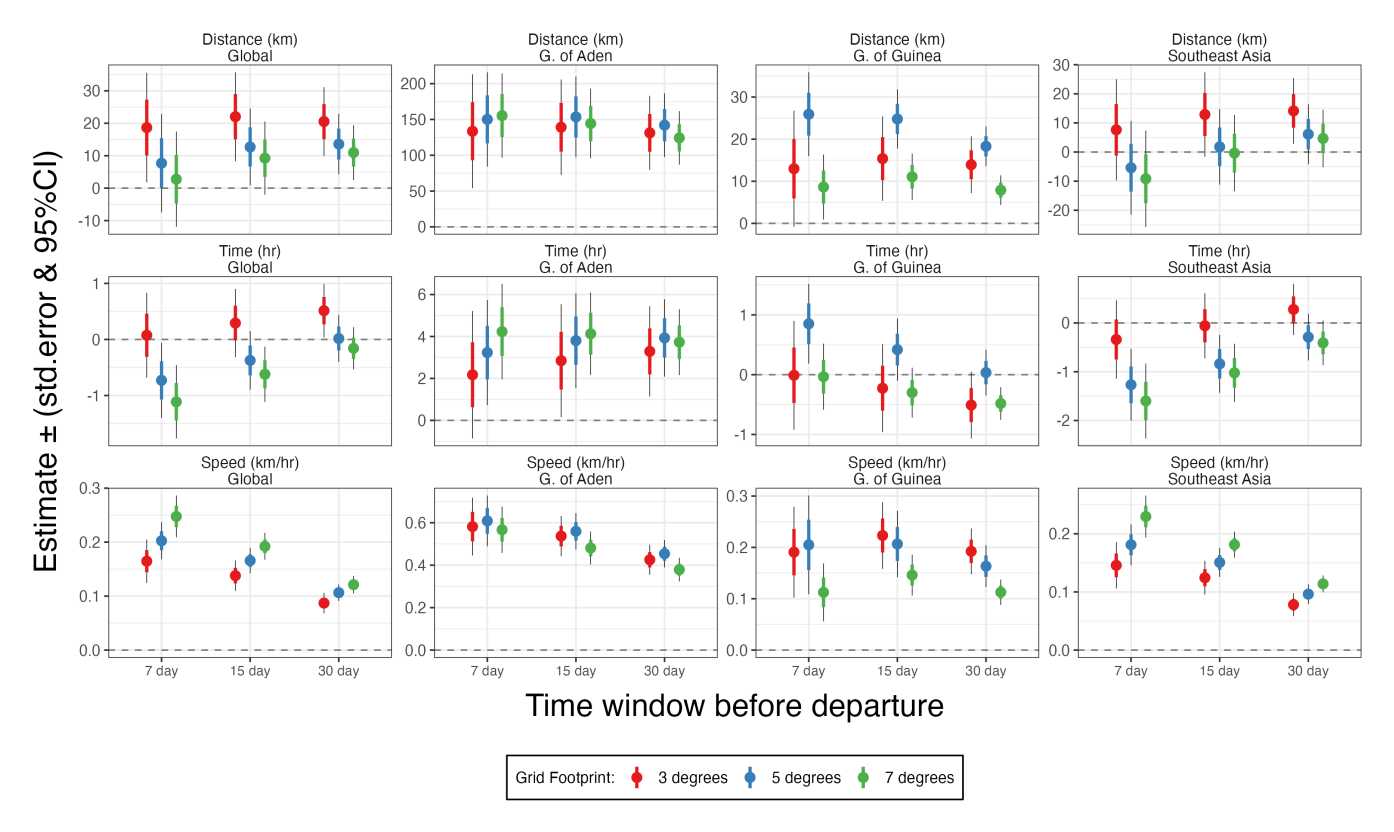


Figure D.6: Replication Using Average Number of Encounters Under Different Time Horizons and Degree Footprints. Coefficients show the change in voyage features as a function of the average number of pirate encounters experienced by other vessels in the preceding months. The analysis is conducted for all the variables and subsamples reported in the main text. Each plot shows the results for models using time windows of 7, 15, and 30 days, respectively. Each color shows results for models using a 3, 5, and 7° spatial footprint, respectively. The thick portion of error bars are the clustered standard errors, and the thin portion of error bars shows 95%CIs. Other than the explanatory variable, estimation, subsampling, specification, and clustering approach remain identical to those in Table 1.

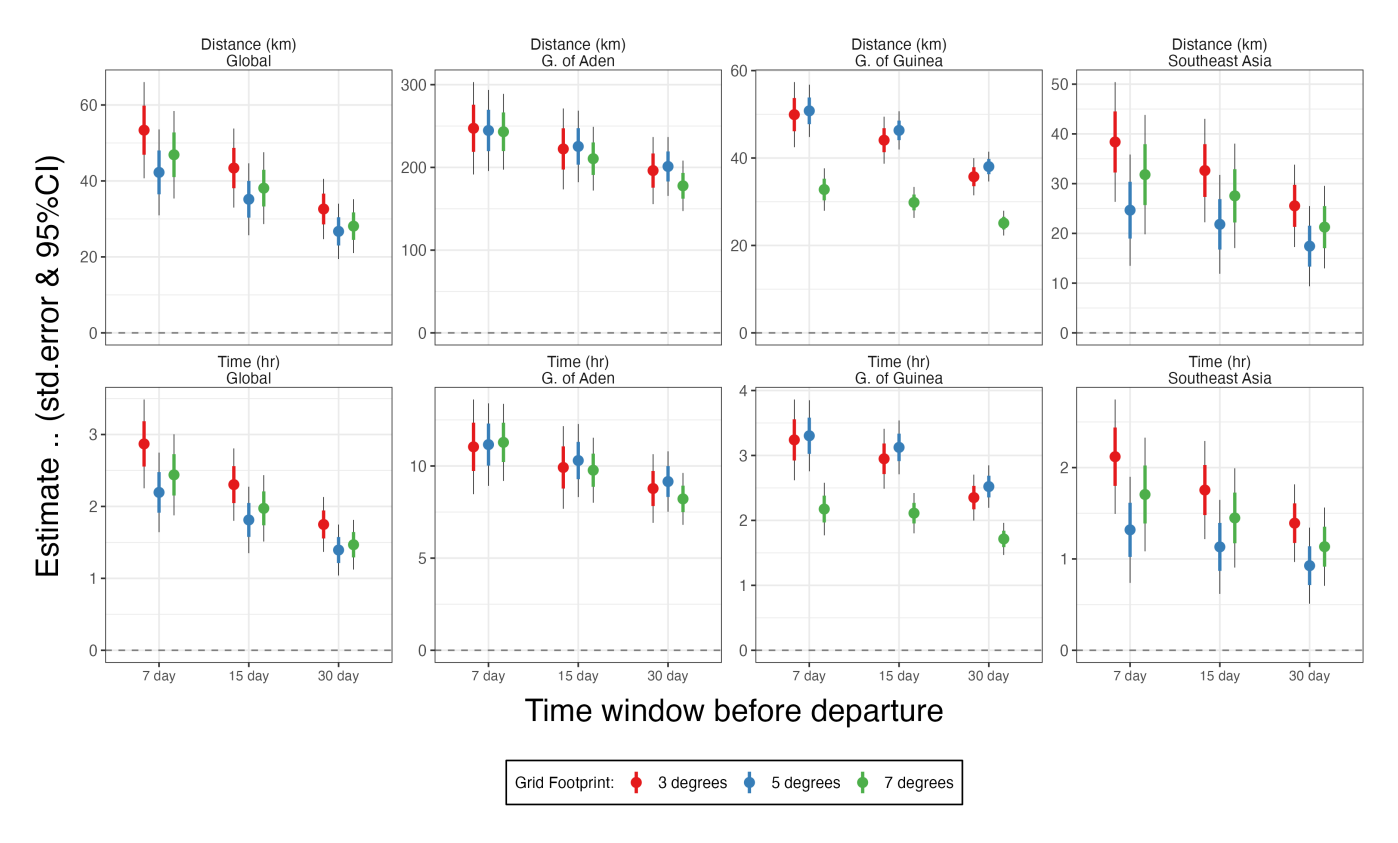


Figure D.7: Replication Using Speed and Days Since Last Encounter as Covariates Under Different Time Horizons and Degree Footprints. Coefficients show the change in voyage features as a function of the average number of pirate encounters experienced by other vessels in the preceding months. The analysis is conducted for all the variables and subsamples reported in the main text. Each plot shows the results for models using time windows of 7, 15, and 30 days, respectively. Each color shows results for models using a 3, 5, and 5° spatial footprint, respectively. The thick portion of error bars are the clustered standard errors, and the thin portion of error bars shows 95%CIs. Other than the explanatory variables, estimation, subsampling, specification, and clustering approach remain identical to those in Table 1.